European Journal of Soil Science

WILEY

European Journal of Soil Science

RESEARCH ARTICLE OPEN ACCESS

How Rilling and Biochar Addition Affect Hydraulic Properties of a Clay-Loam Soil

Vincenzo Bagarello[1] | Pellegrino Conte[1] | Vito Ferro[1,2] | Massimo Iovino[1] | Calogero Librici[1] | Alessio Nicosia[1] | Vincenzo Palmeri[1,2] | Vincenzo Pampalone[1] | Francesco Zanna[1]

[1]Department of Agricultural, Food and Forest Sciences, University of Palermo, Palermo, Italy | [2]NBFC, National Biodiversity Future Center, Palermo, Italy

Correspondence: Alessio Nicosia (alessio.nicosia@unipa.it)

Received: 31 May 2024 | **Revised:** 4 November 2024 | **Accepted:** 12 December 2024

Funding: This work was supported by the Project 'Indagine di laboratorio e di pieno campo sull'uso di Ammendanti naturali dei Suoli per strategie di Conservazione dell'Acqua e dei Nutrienti' (ASCAN)—National Research Centre for Agricultural Technologies, Codice progetto CN00000022, Bando a Cascata Spoke n. 6, CUP D13C22001330005—PRJ-1815.

Keywords: biochar | hydrological connectivity | nuclear magnetic resonance | relaxometry | rill erosion | soil hydrological properties

ABSTRACT

Rill erosion is a significant problem worldwide as it determines relevant amounts of soil loss on hillslopes. Although, in the last few years, many studies have focused on rill erosion and biochar as soil amendment, their influence on soil hydrological properties and relevance on soil conservation strategies is still uncertain. In this paper, the effects of rill formation and biochar addition on the physical and hydraulic properties of a clay-loam soil were assessed by laboratory measurements (water retention, hydraulic conductivity, minidisk infiltrometer data and ^{1}H Nuclear Magnetic Resonance (NMR) relaxometry with the fast field cycling (FFC) setup) and field tests (rill formation tests at the plot scale). The rilled and non-rilled soils did not show any difference in the volume of pores with a diameter (d) > 300 μm, but the former showed a smaller volume for the pores in the size range between 300 and 0.2 μm. As compared with an untreated rilled soil, the addition of 5% (w w^{-1}) biochar in the soil in which the rill is incised did not change the volume of pores with d > 300 μm, while there were more pores of both 30 ≤ d ≤ 300 μm and 0.2 ≤ d ≤ 30 μm. Moreover, there were less pores with d < 0.2 μm. Shaping the rill did not influence the hydraulic conductivity of the nearly saturated soil (pressure head, h = −1 cm), while it determined a significant decrease of the soil ability to transmit water in more unsaturated conditions (h ≤ −3 cm). The addition of biochar to the soil improved, in general, the soil aptitude to transmit water, regardless of the pore size. However, this improvement was statistically irrelevant in the case of a transport process governed by larger pores. The hydrological measurements also demonstrated that the addition of a large amount of biochar (5%) impedes soil characteristics alteration as the changes due to rilling are balanced by adding biochar in the soil. NMR was also used to measure the structural and functional connectivity of the original soil, the biochar and a mixture with three biochar concentrations (i.e., BC = 1%, 3% and 5% w w^{-1}) traditionally applied in agronomical activity. These measurements revealed that the mixture of soil and biochar was characterised by longitudinal relaxation time (T_1) values, which are related to pore sizes, longer than those measured for the soil. In addition, the soil empirical cumulative frequency distribution of T_1 was always skewed towards shorter T_1 values, thereby suggesting that the macro-pore component (i.e., the largest T_1 values) was never dominant while biochar addition increased the size of mesopores and micropores. Biochar concentrations larger than 3% (w w^{-1}) did not produce appreciable changes in the pore distribution inside the mixture. The biochar component improved the structural connectivity up to BC = 5%, while decreased the functional connectivity up to BC = 3%. A relationship between the water volume contained in soil pores and the NMR data were established for the micropores (d ≤ 0.2 μm). The biochar-amended soil was characterised by fewer small pores, but these micropores were greater than those in non-treated soil.

Summary

- Effect of rilling and biochar on soil physical and hydraulic properties is measured.
- Rilling does not influence the hydraulic conductivity of the nearly saturated soil.
- Rilling decreases the soil ability to transmit water in more unsaturated conditions.
- Biochar improves the soil aptitude to transmit water regardless of the pore size.

1 | Introduction

Soil erosion is a relevant environmental problem whose effects are often underestimated although its importance is highlighted in many field investigations (Borrelli et al. 2017). The soil loss rate in agricultural land is estimated as 10–40 times faster than the rate of soil formation, while slope protection is often inadequate and strategies to mitigate or even prevent hydrogeological risk are rare (Carollo et al. 2023).

The evaluation of the link between soil physical and hydraulic properties and soil erosion process is a complex subject as soil physical and hydraulic properties have to be determined for parameterizing soil erosion prediction models (Risse, Nearing, and Savabi 1994; Risse, Nearing, and Zhang 1995; Nearing et al. 1996; Morgan and Duzant 2008). Moreover, generally, these investigations are experimentally rather complex as intensive soil physical and hydraulic characterisation, and the monitoring of surface runoff and soil erosion processes have to be performed at the same time. Perhaps, this is one of the reasons why the direct measurements of the soil hydraulic properties in relevant contexts from a soil erosion point of view are not widely reported in the literature.

Rill erosion is caused by soil particle detachment and transport by channelised flows which are characterised by high flow shear stresses and velocities, which lead to an increased sediment yield. Rills are small-eroded channels, which rapidly change their own morphology, represent a relevant sediment source producing most of the sediment transport on hillslopes (Mutchler and Young 1975; Zhang et al. 2016), and can have a very appreciable impact on the hydrological response of the field in its entirety. Quite surprisingly, despite the hydrological relevance of the small field portions interested by rills, studies about the differences between the hydraulic properties of the rilled and non-rilled soils are lacking.

In a context in which alternative soil conservation practices aimed at the limitation of soil erodibility appear to be a valid solution to mitigate erosion processes, organic amendments, such as biochar (Mukherjee, Lal, and Zimmerman 2014) or compost (Chia et al. 2020), can be considered as a valid and eco-friendly solution for soil amendment.

Biochar is obtained from the pyrolysis (i.e., thermal degradation) of biomasses in oxygen-starved conditions (Sohi et al. 2010; Conte et al. 2021). It improves soil structure (size, arrangement and aggregate stability) (Blanco-Canqui 2017; Conte et al. 2021), increases its organic matter content, and determines an increase in crop yield and quality (Wang and Wang 2019; Conte et al. 2021). However, contrasting effects of biochar addition on runoff and soil loss have been reported since some authors (Lee et al. 2018; Li et al. 2017, 2019; Zhang et al. 2019) concluded that biochar addition can promote soil loss, while other investigations (Abrol et al. 2016; Baiamonte et al. 2015; Doan et al. 2015; Hseu et al. 2014; Jien and Wang 2013; Lee et al. 2015; Sadeghi, Hazbavi, and Harchegani 2016; Smetanová et al. 2013) supported the hypothesis that this addition reduces soil susceptibility to erosion. Moreover, the existing literature pointed out that the biochar effectiveness is influenced by the added concentration. Some authors (Li et al. 2019, 2020) suggested that low (from 1% to 3%) and high *BC* (higher than 5%) values generally inhibited and promoted soil loss, respectively, while the results of the meta-analysis by Gholamahmadi et al. (2023) indicated the limit of 2.5% w w^{-1} by considering that it seems that larger *BC* have no effect on the reduction of soil loss.

These contrasting results can be justified by several effects: (i) differences due to the biochar type and its particle size; (ii) changes in physical and chemical properties of investigated soils; (iii) the vegetation growth; and (iv) the method used for adding biochar (spread over the soil surface, incorporated into the soil) (Wani et al. 2021). In particular, when biochar was spread on the soil surface (Sadeghi, Hazbavi, and Harchegani 2016; Smetanová et al. 2013), a biochar surficial layer forms and inhibits seal formation, favours infiltration processes, and reduces runoff and soil loss. Moreover, spreading of biochar on soil surface produces a preferential transport of low-density biochar particles (Sadeghi, Hazbavi, and Harchegani 2016) and a reduction of soil loss. However, biochar is usually applied in the field inside the arable soil horizon and thoroughly mixed to favour the effects on soil properties.

At present, most of the literature studies deal with interrill erosion processes due to simulated rainfalls, while few investigations on rill erosion are available (Li et al. 2021; Nicosia, Pampalone, and Ferro 2021). Li et al. (2021) carried out some experimental runs on the susceptibility to rill formation, and they observed a decrease in rilling in biochar-amended soil. Nicosia, Pampalone, and Ferro (2021), using the data collected by Li et al. (2021), demonstrated that the biochar addition led to an increase in roughness, which determined the decrease in flow velocity and the increase in water depth. Parhizkar et al. (2023) studied the effect of rice husk-biochar on rill erosion by flume experiments with both not amended soil and soil with a *BC* of 3% w w^{-1}. The measurements revealed that biochar reduced rill erodibility and critical shear stress for the investigated soil. Furthermore, Parhizkar et al. (2023) found greater stability of the aggregates and a lower bulk density of the treated soil as compared to the non-amended one.

Biochar application influences soil porosity via direct pore contribution from pores within the biochar, creation of packing or accommodation pores between biochar and the surrounding soil aggregates, improved persistence of soil pores due to increased aggregate stability, increased bioturbation such as earthworm activity (Hardie et al. 2014; Blanco-Canqui 2017). According to Hardie et al. (2014), who worked on a sandy-loam soil, large

macropores (> 1200 μm) can be formed due to a greater earthworm burrowing in the biochar-amended soil. In clayey soils, biochar may favour the formation of mesopores (Lu, Sun, and Zong 2014). For loamy-sand soils, small particles of biochar (< 500 μm) can reduce the volume of small pores (diameter < 0.5 μm) and fissures (> 500 μm) while can increase the volume of pores in the range 0.5–500 μm (Głąb et al. 2016). With reference to coarse soils, biochar addition might convert large pores into smaller pores (Petersen et al. 2016; Villagra-Mendoza and Horn 2018).

Biochar addition can also be expected to variably influence soil water transmission properties. For example, different biochar treatments could not have any statistically significant effect on saturated soil hydraulic conductivity, K_s, in clay (Castellini et al. 2015) and loamy-sand soils (Głąb et al. 2016). However, the fill in of larger pores due to biochar addition in coarse-textured soils can be expected to decrease K_s and increase the unsaturated soil hydraulic conductivity (Villagra-Mendoza and Horn 2018).

An increase in field studies on biochar, the need to focus less on the effects and more on the mechanisms by which biochar application alters soil physical properties, and more research on biochar benefits in degraded or problematic soils are some of the research needs on biochar application that were identified only a few years ago (Blanco-Canqui 2017).

The word 'connectivity' states the way in which an environmental system favours matter and energy movement inside or among its elements (Pringle 2003; Bracken and Croke 2007; Marchamalo, Hooke, and Sandercock 2016; Keesstra et al. 2020). This concept highlights the attitude of a vector, such as water, to transport materials at different spatial and temporal scales (Bracken et al. 2013; Reaney, Bracken, and Kirkby 2014; López-Vicente, Nadal-Romero, and Cammeraat 2017), considering the heterogeneity and complexity of an environmental system.

Wainwright et al. (2011) proposed to characterise an environmental system by structural (*SC*) and functional (*FC*) connectivity. The first one (*SC*) represents how the investigated process is affected by the interactions among structural characteristics of the environmental system (Belisle 2005; Turnbull, Wainwright, and Brazier 2008; Baartman et al. 2013; Uezu, Metzger, and Vielliard 2005). For example, this is the case when the focus is to establish how the grain size distribution and arrangement of soil particles affect water movement inside the soil. The second one (*FC*) represents how a specific process (e.g., hydrological) is affected by the interactions among the structural components of the investigated system and the vector (e.g., water) (Wainwright et al. 2011). According to these definitions, structural connectivity provides a time-independent (stationary) response of the examined system, while functional connectivity reflects a dynamic viewpoint.

Conte and Ferro (2018, 2020, 2022) proposed the concept of *hydrological connectivity inside the soil* (*HCS*) to represent how water movement inside the soil is affected by the interaction of soil spatial patterns (i.e., *SC*) with chemical and physical processes (i.e., *FC*). In this system, the structural connectivity represents the spatial distribution of soil particles and considers the spatial arrangement of soil pores and micro-channels, while the functional connectivity complies with the water movement inside soil pores and is related to the physical–chemical interactions of water with the pore edges (Conte et al. 2017).

The scientific gaps to overcome concerns the definition of the threshold value of biochar concentration useful for soil conservation strategies and understanding the connectivity of biochar-amended soils.

In this paper, experimental measurements performed on rills of a clay-loam soil amended with different concentrations of biochar are aimed to: (i) investigate how the soil hydrological properties of the rilled soil with different biochar concentrations (*BC* = 0%, 3% and 5%) change in comparison with the original soil; (ii) assess, by the nuclear magnetic resonance (NMR) relaxometry with the fast field cycling (FFC) layout, the structural and functional connectivity of the original soil, the biochar and mixtures with different biochar concentrations (*BC* = 1%, 3% and 5% w w^{-1}); (iii) test if the increase of *BC* produces appreciable changes in the pore distribution inside the mixture; and (iv) combine hydrological and NMR measurements to establish a relation between the water volume contained in different-sized soil pores, and their number and size.

2 | Materials and Methods

2.1 | Experimental Setup

The experimental measurements were performed on a plot, which is a large box (Figure 1) 2 m wide and 7 m long, located at the Department of Agricultural, Food, and Forest Sciences (AFFS) of the University of Palermo (38° 06′ 25″ N, 13° 20′ 59″ E). The plot is manually filled with a clay-loam soil (32.7% clay, 30.9% silt and 36.4% sand), which is the same already used by Carollo et al. (2021), Di Stefano et al. (2022), and Nicosia et al. (2022a, 2022b), compacted at the field bulk density and with an average slope of 15%. The soil depth in the plot ranges from 0.45 m (upstream end) to 0.15 m (downstream end). This soil was taken in the area surrounding the Department, which is characterised by a typical Mediterranean climate *Csa*, according to the Köppen classification (Köppen 1918) and vegetation. The soil was collected from different points within the area to consider field variation. The abovementioned soil texture was determined by the hydrometer method (Kroetsch and Wang 2008) for fine size fractions and mechanical dry sieving for coarse fractions, applied to five samples homogeneously distributed on the plot surface. Other five soil samples were collected by steal cylinders of known dimensions (5 cm in height and 5 cm in diameter) to determine bulk density (1.23 g cm-3) (Hao et al. 2008), by oven-drying at 105°C for 24 h. The organic matter content of the soil, determined by oven-drying the samples in a muffle furnace at 400°C (Skjemstad and Baldock 2008), is approximately equal to 2%. Two trenches (Figure 1a), 5.7 m long, 0.2 m wide and 0.1 m deep, were dug in the plot for a total removal of approximately 100 kg of soil for each of them. The soil removed from each trench was distributed on plastic sheets in piles and left to air-dry for a week. At the end of the week, three samples

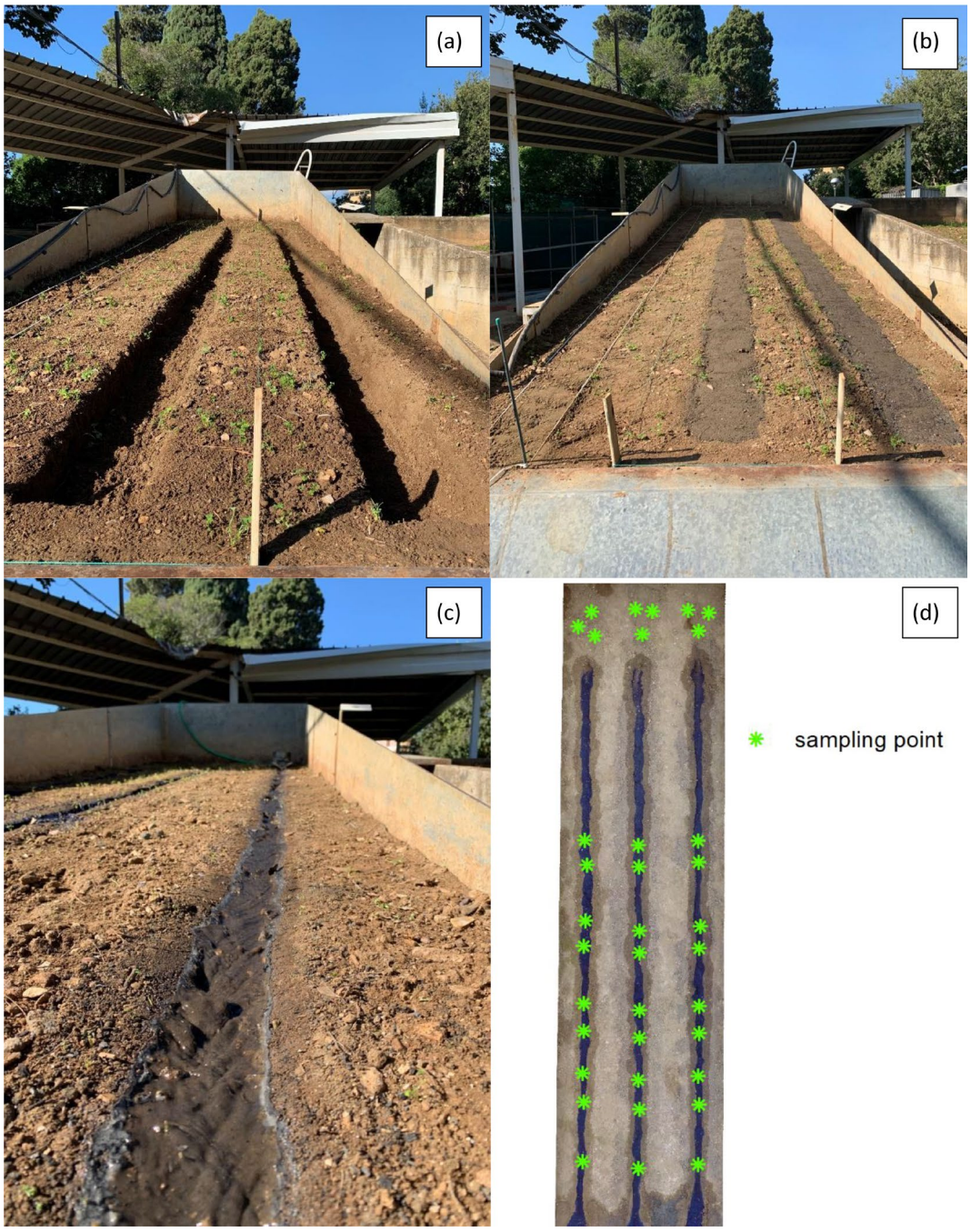

FIGURE 1 | View of the experimental plot with the two empty (a) and filled trenches (b), the preferential paths (c) and scheme of the sampling points (d).

were taken and weighted from each pile, and they were subsequently oven-dried at 105° for 24 h to determine soil moisture, which was found to be on average 12.5% ± 0.004%. The pre-established *BC* of 3% (B_3 treatment) and 5% (B_5 treatment) was reached by adding 300 and 500 g of biochar to 10 kg of soil in dry weight, corresponding to approximately 11.4 kg in wet weight, due to the measured soil moisture. The mixing phase between soil and biochar was performed for 60 s. Each biochar-soil mixture corresponding to an investigated *BC* (3% and 5%) was used to fill a trench (Figure 1b). The experimental runs were carried out after an incubation period of 30 days to allow biochar incorporation into the soil. Two preferential paths were established on the surface of the two filled trenches (B_3 and B_5 treatment) and modelled by a constant clear inflow discharge of 0.33 L s^{-1} (Figure 1c) applied for 12 min to simulate rilling. A preferential flow path, evolving in a rill during the run, was also established in a zone of the plot in which the soil was not treated with biochar (B_0 treatment) (Figure 1b) as control. The same discharge of 0.33 L s^{-1} was applied for 12 min.

2.2 | Hydrological Measurements

After the rilling, the surface soil was sampled in four zones of the plot (Figure 1d) using stainless steel cylinders (diameter = 0.05 m, height = 0.05 m) to collect undisturbed soil cores. In

particular, for each rill (B_0, B_3 and B_5 treatments), a total of nine soil cores were collected along the rill in correspondence of the sampling points shown in Figure 1d. The other nine soil cores were randomly collected in the upper plot area (Figure 1d), in a zone without rills and where biochar was not added (C treatment). Therefore, a total of 36 undisturbed soil cores were collected.

Water retention data were obtained for each undisturbed soil core for pressure head, h, values of 0, −0.05, −0.075, −0.10, −0.15, −0.20, −0.25, −0.30, −0.40, −0.50, −0.70 and −1.0 m by a self-made hanging water column apparatus (Bagarello and Iovino 2012; Bondì, Castellini, and Iovino 2022). The apparatus consists of an array of 40 glass funnels, each equipped with a sintered porous plate having an air entry value of −2.0 m that is connected to a graduated burette, which can be moved in height to establish a given pressure head value and allows measurement of the drained water from the core. The cores were previously saturated on the porous plate by wetting from below and then equilibrated at decreasing h values. The dry soil bulk density, ρ_b, and the volumetric water content corresponding to the last equilibrium pressure head value were determined by oven-drying the core. The volume of water drained into the burette was recorded and used to calculate the volumetric water content corresponding to the equilibrium pressure heads.

The oven-dried soil cores were placed for several days in a large container containing a few small plastic cups with water. For a given (negative) h value, the hydraulic conductivity, K, of a soil core was then determined by a simplified version of the Unit Hydraulic Gradient (UHG) method (Klute and Dirksen 1986; Bagarello, Castellini, and Iovino 2007). In particular, to establish a given h value at the base of the core, a plastic box of 38 (length) × 17 (width) × 13 (height) cm^3 was filled with a bed of sand up to a certain height, and several small holes were made on the walls of the box at a downward distance h (L) from the surface of the sand bend. A metal screen was glued to each hole to prevent sand from escaping through the hole. Water was added to the box so as to form a saturated zone below the holes and an unsaturated zone above them. At hydrostatic equilibrium, the soil water pressure head at the surface of the sand bed was assumed to be equal to h. Different boxes were prepared, depending on the considered h value ($h = -6$, −3 and −1 cm in this investigation). The soil core, with an attached nylon guard cloth at its base to prevent soil loss from the bottom, was placed on the surface of the sand box and left to equilibrate for several days. Small volumes of water were periodically added to the box during this period to maintain the h value at the surface of the sand bed constant. Then, a Mini-Disk Infiltrometer (MDI), set at the same h value of the sand surface, was placed on the top of the soil core, and a one-dimensional infiltration process was activated. When necessary, small amounts of loose soil were applied to the soil surface of the core to improve the contact between the device and the soil. The first established pressure head was $h = -6$ cm. At the end of the run, the soil core was subjected to the subsequent step by imposing the higher h value of the sequence. Readings at the MDI reservoir were taken visually at 0.5–5 min time intervals, depending on the imposed pressure head and the stage of the run.

After drying, the soil was used to prepare packed soil samples (diameter = 0.05 m, height = 0.01 m) at the same bulk density of the soil core. In particular, a pestle was gently used to crush the soil, which was then passed through a 2 mm sieve. These soil samples were used to determine the soil water content corresponding to h values of −10 and −150 m by a pressure plate apparatus (Dane and Hopmans 2002).

2.3 | Soil Water Retention and Hydraulic Conductivity Data

Four points of the water retention curve were considered to establish comparisons between the four treatments (C, B_0, B_3, B_5), in accordance with Reynolds et al. (2009). These points corresponded to pressure heads of 0, −0.1, −1 and −150 m. Consequently, the saturated soil volumetric water content, θ_s (m^3/m^3), the 'saturated' volumetric water content of the soil matrix, $\theta_{-0.1m}$ (m^3/m^3), the field capacity volumetric soil water content, θ_{-1m} (m^3/m^3), and the permanent wilting point volumetric soil water content, θ_{-150m} (m^3/m^3) were considered. According to Hardie et al. (2014), the Young-Laplace equation can be used to determine the size of the largest pores that are full of water for a given absolute value of the soil water pressure head, h (m):

$$d = \frac{30}{|h|} \tag{1}$$

where d (μm) is the pore diameter. All pores are full of water for $\theta = \theta_s$. The d values are equal to 300, 30 and 0.2 μm for $h = -0.1$, −1 and −150 m, respectively. Equivalent pore diameters ≤ 300 μm ($h \leq -0.1$ m) comprise the soil matrix domain, while diameters > 300 μm ($h > -0.1$ m) form the macropore domain (Topp et al. 1997; Jarvis et al. 2002; Reynolds et al. 2002).

Soil air and water storage capacities were expressed by distinguishing between pore sizes (Reynolds et al. 2002, 2009). In particular, macroporosity, equal to $(\theta_s - \theta_{-0.1m})$, gives the total volume of large (macro) pores (i.e., > 300 μm equivalent pore diameter), which indicates, albeit indirectly, the soil's ability to quickly drain excess water and facilitate root proliferation. According to Reynolds et al. (2009), macroporosity is optimal if $(\theta_s - \theta_{-0.1m}) \geq 0.07\ m^3/m^3$, intermediate if $0.04 \leq (\theta_s - \theta_{-0.1m}) < 0.07\ m^3/m^3$, and limited if $(\theta_s - \theta_{-0.1m}) < 0.04\ m^3/m^3$. The $(\theta_{-0.1m} - \theta_{-1m})$ difference ($30 \leq d \leq 300$ μm) is expressive of soil aeration in the soil matrix domain (Reynolds et al. 2002). As suggested by Reynolds et al. (2002), aeration of soil matrix is good if $(\theta_{-0.1m} - \theta_{-1m}) \geq 0.10$–$0.15\ m^3/m^3$ and is limited for smaller values. The $(\theta_{-0.1m} - \theta_{-1m})$ difference was denoted as drainable porosity and corresponds to the −1.0 to −10 kPa matric pressure considered in other investigations specifically focused on biochar addition effects on soil water retention (Hardie et al. 2014). The plant-available water capacity, equal to $(\theta_{-1m} - \theta_{-150m})$ ($0.2 \leq d \leq 30$ μm), represents the plant available water capacity (Reynolds et al. 2002). According to Reynolds et al. (2009), water availability is ideal if $(\theta_{-1m} - \theta_{-150m}) > 0.20\ m^3/m^3$, good if $0.15 \leq (\theta_{-1m} - \theta_{-150m}) < 0.20\ m^3/m^3$, limited if $0.10 \leq (\theta_{-1m} - \theta_{-150m}) < 0.15\ m^3/m^3$ and poor if $(\theta_{-1m} - \theta_{-150m}) < 0.10\ m^3/m^3$.

The S index by Dexter (2004) was also calculated to evaluate the soil physical quality (SPQ) of the sampled soil by considering the soil water retention curve expressed in terms of gravimetric soil water content θ_g (g/g). In particular, the van Genuchten (1980) model was adapted to the measured data:

$$\theta_g(h) = \theta_{gr} + (\theta_{g\theta s} - \theta_{gr})\left(1 + |\alpha h|^n\right)^{-nm} \quad (2)$$

in which θ_{gs} (g/g) and θ_{gr} (g/g) are respectively the saturated and residual gravimetric water content, α (1/cm) is a scale parameter, and n and m (with $m = 1–1/n$) are shape parameters. Equation (2) was adapted to the data by optimising the parameters θ_{gr}, α and n. The calculation of S was performed according to the following equation (Reynolds et al. 2009):

$$S = \left| -n\left(\theta_{gs} - \theta_{gr}\right)\left[1 + \frac{1}{m}\right]^{-(m+1)} \right| \quad (3)$$

The S index represents the magnitude of the slope of the soil water retention curve at the inflection point when the curve is expressed as gravimetric water content versus natural logarithm of the pore water tension head. According to Dexter and Czyż (2007), $S \geq 0.050$ indicates 'very good' soil physical or structural quality, $0.035 \leq S < 0.050$ is indicative of a 'good' physical quality, $0.020 \leq S < 0.035$ suggests a 'poor' physical quality and $S < 0.020$ denotes a 'very poor' or 'degraded' physical quality. This evaluation criterion does not appear to have universal validity since large S values can also be expected to reflect the soil matrix characteristics rather than the soil structural characteristics (Reynolds et al. 2009). For this purpose, Dexter et al. (2008) reported that large apparent values of S, which are not reflected in other physical properties, can be obtained in well-graded sands and sandstones that have a very narrow distribution of pore sizes and can empty over a very narrow range of suctions. Nevertheless, the S index is largely used, probably because it allows for defining the SPQ on the basis of a single value that is expressive of a robust experimental information, given that determining S requires adapting a model to the experimentally determined water retention data. In particular, this index was taken into consideration in several investigations testing the impact on SPQ of various amendments, including biochar (Reynolds et al. 2009; Gląb et al. 2016; Dokoohaki et al. 2017; Fouladidorhani et al. 2023).

For each soil core and each pressure head value, the cumulative infiltration, I (mm), versus time, t (h), relationship obtained with the MDI was linear or nearly linear from the early stage of the run, suggesting a rapid stabilisation of the flow process. Therefore, an estimate of K was obtained by considering the complete infiltration run and determining by linear regression the slope of the I versus t relationship forced to pass through the origin of the axes. As an example, Figure 2 shows, for the run no. 7 of the B_0 treatment, the I (t) data points for the three established pressure heads (−6, −3 and −1 cm) and the corresponding estimates of K coinciding with the slopes of the fitted linear regression lines. The coefficient of determination, R^2, of these relationships was >0.99. The symbols K_{-6cm}, K_{-3cm} and K_{-1cm} were used to denote the K values corresponding to $h = -6$, −3 and −1 cm, respectively.

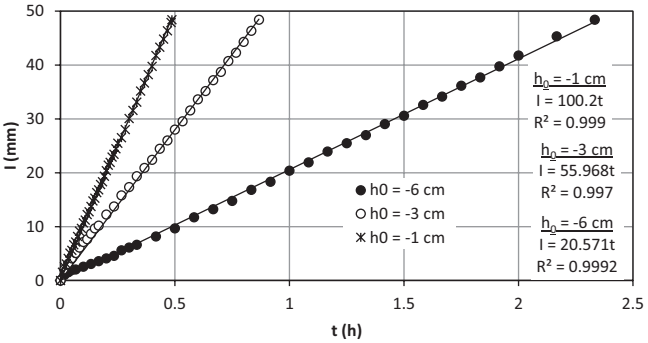

FIGURE 2 | Example of the applied procedure to determine the soil hydraulic conductivity at a given pressure head, h_0, from the MDI runs (I = cumulative infiltration; t = time).

2.4 | Hydrological Data Analysis

Initially, rilling effects on soil physical and hydraulic properties were tested by comparing the C and B_0 treatments. Then, biochar addition effects on the soil of a rill were tested by comparing the B_0, B_3 and B_5 treatments.

For each tested effect, comparisons were performed by considering the following variables: ρ_b, θ_s, $\theta_{-0.1m}$, θ_{-1m}, θ_{-150m}, $(\theta_s - \theta_{-0.1m})$, $(\theta_{-0.1m} - \theta_{-1m})$, $(\theta_{-1m} - \theta_{-150m})$, S, K_{-6cm}, K_{-3cm} and K_{-1cm}. An F test and a two-tailed t test at $p = 0.05$ were applied to establish the statistical significance of the differences. At this aim, the statistical functions for data analysis of the Excel spreadsheet (Microsoft Corporation, Redmond, WA) were used.

Finally, an attempt to describe the combined rilling and biochar addition effects was made by considering four measured points of the water retention curve (θ_s, $\theta_{-0.1m}$, θ_{-1m}, θ_{-150m}), the S index obtained from the complete water retention dataset for a core, and also K for the three pressure heads (K_{-6cm}, K_{-3cm}, K_{-1cm}).

2.5 | Sample Preparation for FFC NMR Relaxometry Analyses

All the soil samples were weighed (≈2 g) in a 10 mm NMR glass-tube. Then, MilliQ grade water (18.2 MΩ cm at 25°C) was gradually added till saturation occurred. The samples were kept overnight and, finally, analysed with the NMR machine described below.

2.6 | FFC NMR Relaxometry Experiments

A Stelar SmarTracer Fast-Field-Cycling NMR Relaxometer (Stelar s.r.l., Mede, PV–Italy) at a constant temperature of 25°C was used to carry out the relaxometry experiments. The basics of the FFC NMR relaxometry are reported elsewhere (Conte and Lo Meo 2020). Briefly, the technique is based on the rapidly switching among three different magnetic fields, that are referred to as polarisation (B_{POL}), relaxation (B_{RLX}) and acquisition (B_{ACQ}) field. In the non-polarised (NP) configuration, B_{POL} intensity is kept null. Therefore, only B_{ACQ} and B_{RLX} are

used. The former is applied to generate the magnetization whose intensity depends on that of B_{ACQ} which is changed in the proton Larmor frequency (ν_L) interval 0.01–10 MHz. The intensity of the latter (i.e., B_{ACQ}) was set at the constant ν_L value of 7.2 MHz. This was needed to keep the magnetization aligned along the $+y$-axis after the application of a ^1H $90°_{(-x)}$ pulse of 6.6 μs necessary to generate the observable and, hence, to allow signal acquisition. B_{ACQ} duration (usually indicated with the Greek letter τ) was logarithmically changed at least 32 times between a minimum given by $0.01 \bullet T_1^*$ and a maximum given by $4 \bullet T_1^*$. Here, T_1^* represents the supposed longitudinal relaxation time of the system under study (Conte 2021). The aforementioned 32 τ values were automatically calculated by the software (AcqNMR95, V. 2.20, 2007) provided with the NMR machine. When B_{RLX} Larmor frequency became ≤ 3 MHz, the pre-polarised (PP) configuration was used. In other words, B_{POL} intensity was set to be non-null. The B_{POL} intensity (expressed as proton Larmor frequency) used in the present study was 10 MHz. It was applied for a period of time (also referred to as T_{POL}) given by $4 \bullet T_1^*$, having T_1^* the same meaning reported above. The necessity of the PP configuration lies in the fact that when B_{RLX} $\nu_L \leq 3$ MHz, a lack of NMR sensitivity is achieved. Therefore, the application of a polarisation field prior of B_{RLX} allows sensitivity enhancement and amelioration of FFC NMR data quality (Conte 2021). A recycle delay (RD) of 4 s was applied when either NP or PP configurations have been used. This RD value was long enough to prevent any problem due to signal saturation. Finally, a switching time of 3 ms, an acquisition delay of 8 μs, a receiver inhibit of 15 μs, and a block size of 512 points were used.

2.7 | FFC NMR Relaxometry Data Analyses

Once the FFC NMR relaxometry data have been acquired, the Uniform PENalty regularisation (UPEN) algorithm (Borgia, Brown, and Fantazzini 1998; Conte 2019) was used to achieve the distribution of the longitudinal relaxation times to assess the hydrological connectivity inside a soil (HCS).

For each soil, following the result by Conte and Ferro (2020), the distribution of T_1 was obtained using a sample-to-water ratio of 1:0.25 (w/w), corresponding to the water holding capacity *WHC*, at a proton Larmor frequency ν_L varying from 0.01 to 10 MHz. In other words, the experimental runs were carried out with a single value of *WHC* and different values of ν_L. Each sample was prepared in a beaker, and then the wet sample was manually transferred in the NMR tubes to obtain a homogeneous packing. The FFC NMR measurements were carried out for the original soil (C treatment), the biochar, and the mixtures with different biochar concentrations (1%, 3% and 5%, that is, B_1, B_3 and B_5 treatments). Three replicates of NMR measurement were carried out for each investigated sample.

2.8 | Assessing Hydrological Connectivity Inside a Soil (HCS)

NMR relaxometry measures how quickly the z-component of the nuclear magnetic moment (i.e., the bulk nuclear spin magnetization) changes from a non-equilibrium state to the equilibrium distribution. Fluctuations of local magnetic or electrical fields generate a phenomenon, named relaxation, which is mainly affected by molecular motions. Therefore, measurements of the longitudinal relaxation time, T_1, express the molecular dynamics. The T_1 values provide information about motion frequencies in the range (10^5–10^8 Hz) characteristic of water molecules moving in porous media (Conte 2021). If the porous medium is the soil, the shortest T_1 values are associated with small-sized pores (i.e., pores bounded by clay primary particles and small aggregates), while the longest T_1 values correspond to pores bounded by sand particles, silt and large aggregates (Pohlmeier, Haber-Pohlmeier, and Stapf 2009; Conte et al. 2017).

Water molecules moving within the micro-pores have a range of T_1 values (T_A in Figure 3b) near the lower T_1 limit, while molecules moving within the macro-pores are characterised by T_1 values near the upper T_1 limit (range named T_B in Figure 3b) of the measured relaxation time distribution. Water molecules moving within meso-pores are identified by all T_1 values included between the upper T_1 limit of the micro-pores (point A in Figure 3b) and the lower T_1 limit of macro-pores (point B in Figure 3b).

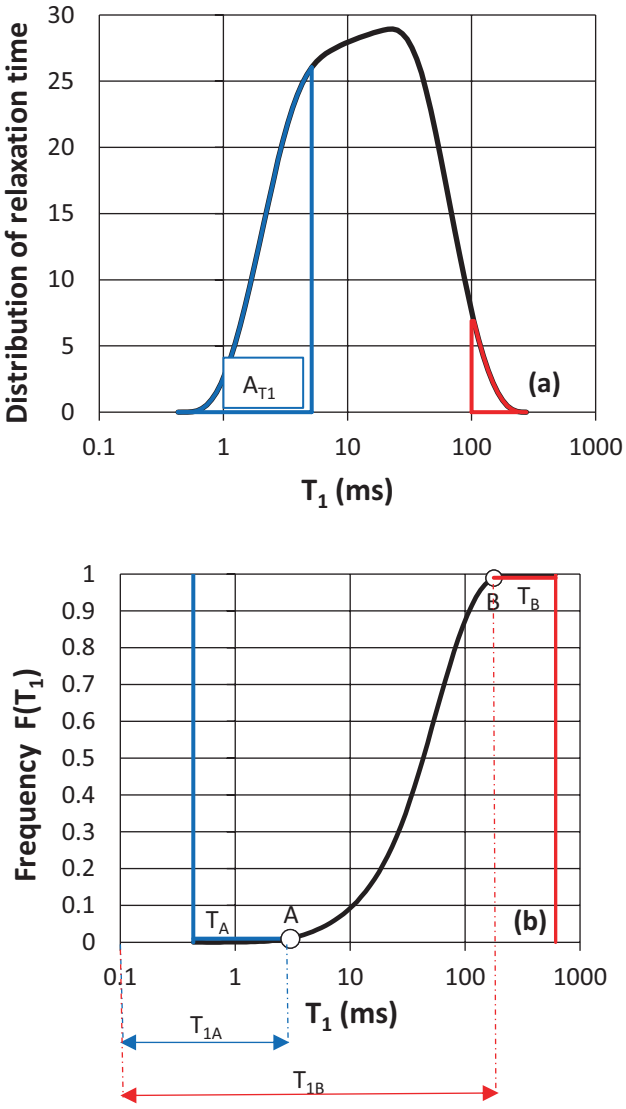

FIGURE 3 | Relaxogram (a) and example of the integral curve of the relaxogram that associates the ratio A_{T1}/A with each T_1 value (b).

Conte and Ferro (2018, 2020, 2022) presented a method for defining the *SC* and *FC* of a given soil by introducing a new mathematical use of the relaxograms obtained by NMR relaxometry. The quantification of structural connectivity and functional connectivity was made by two indexes, *SCI* and *FCI*, calculated by taking into account the NMR relaxogram shapes. In detail, for a given proton Larmor frequency, the distribution of the longitudinal relaxation time T_1 (i.e., the relaxogram in Figure 3a) is integrated, and the area, A_{T1}, bounded by the relaxogram curve, the T_1 axis, and the ordinate value corresponding to T_1 value, is related to each T_1 value. Figure 3b plots an example of the integral curve of the relaxogram, associating the ratio A_{T1}/A with each T_1 value. This ratio, ranging from 0 to 1, is equal to the non-exceeding empirical cumulative frequency, $F(T_1)$, of each T_1 value. Conte and Ferro (2018, 2020, 2022) demonstrated that $F(T_1)$ is S-shaped and found two points (A and B in Figure 3b) characterised by a sudden change in the curve slope. The A point bounds a part of the curve corresponding to the shortest T_1 values and the time range T_A (Figure 3b), while the B one limits the part characterised by the longest T_1 values obtained in the T_B time range. Conte and Ferro (2018, 2020, 2022) set the A and B points to identify the two extreme components of the S-shaped $F(T_1)$ distribution: point A, with ordinate $F(T_1)=0.01$, and point B, with ordinate $F(T_1)=0.99$. The ordinate of point A distinguishes the low component (only 1% of the measured T_1 values are less than the abscissa characterising the A point), whereas the ordinate of the B point distinguishes the high component (only 1% of the measured relaxation times values are higher than the abscissa characterising this point).

The water movement in macropores, mesopores, and micropores is considered by the HCS. Adapting the classification by Reynolds et al. (2009) to this investigation, macropores have a diameter $d>300\,\mu m$, mesopores vary in size between 300 and $0.2\,\mu m$, and micropores have $d\leq 0.2\,\mu m$. Note that this classification is similar to some extent to the one by Russell (1973), distinguishing between coarse ($>200\,\mu m$), medium ($200–20\,\mu m$), fine ($20–2\,\mu m$) and very fine ($<2\,\mu m$) pore width classes. Associating the relaxation times with pore sizes, the low component of the $F(T_1)$ distribution, corresponding to T_1 values lower than the abscissa of the A point (Figure 3b), identifies micro-pores, where limited space causes a reduction of molecular movement. The high component, corresponding to T_1 values higher than the B point abscissa (Figure 3b), is related to macro-pores characterised by wide mobility.

For the NMR analysis, the pore-size ranges suggested by Pagliai and Vignozzi (2002) were applied. In particular, micropores have a diameter less than $50\,\mu m$, mesopores range from 0.5 to $50\,\mu m$, and macropores have $d\geq 50\,\mu m$. Therefore, according to Conte and Ferro (2018), in Figure 3b, the abscissa of the point A (T_{1A}) corresponds to the micropore limit ($d<0.5\,\mu m$), while T_{1B} represents the lower limit of the macropore range ($d\geq 50\,\mu m$). The range between T_{1A} and T_{1B} represents the mesopore size interval. The limit of this approach is the unavailability of a direct relationship between the measured T_1 values (relaxogram) and pore diameter sizes. In other words, a calibration of the relaxogram, where the T_1 scale corresponds to the pore diameter size scale has not been attempted yet.

Bulk water movement, characterised by a high sensitivity by the NMR technique (Conte 2019), is related to the limb of the $F(T_1)$ curve (bounded by the A and B points of Figure 3b), whereas the high and low $F(T_1)$ components refer to water interacting with the soil pore edges.

Conte and Ferro (2018, 2020, 2022) proposed the ratio T_B/T_A as *FCI*. This definition of functional connectivity allows for taking into account that the T_1 values in the range T_A identify water trapped in small pores, whereas those in the range T_B correspond to water contained in large pores. Conte and Ferro (2018, 2020, 2022) proposed to use the AB limb zone of the $F(T_1)$ curve (Figure 3b), falling in the central range of T_1 values, to calculate the *SCI*. In other words, the spatial pattern inside the soil can be represented by the central range of T_1 values, identifying water moving in meso-pores. Considering the relationship between T_1 values and pore size, the *SCI* is the coefficient of variation of T_1 values characterised by $0.01<F(T_1)<0.99$.

3 | Results and Discussion

3.1 | Rilling

The ρ_b values did not differ between the C and B_0 treatments (Table 1). The non-rilled soil had significantly higher θ_s and $\theta_{-0.1m}$, equal θ_{-1m} and smaller θ_{-150m} values as compared with the rilled soil. There was not any statistically significant difference between the C and B_0 treatments with reference to $(\theta_s-\theta_{-0.1m})$ but the former treatment yielded higher $(\theta_{-0.1m}-\theta_{-1m})$ and $(\theta_{-1m}-\theta_{-150m})$ values than the latter one. Regardless of the treatment, data variability was low for ρ_b, θ_s, $\theta_{-0.1m}$, θ_{-1m}, θ_{-150m} and $(\theta_{-1m}-\theta_{-150m})$ and medium for $(\theta_{-0.1m}-\theta_{-1m})$ (Warrick 1998). The variability of $(\theta_s-\theta_{-0.1m})$ was high for the C treatment and medium for the B_0 one.

According to the *S* calculations, the soil had a very good physical or structural quality (Dexter and Czyż 2007), regardless of whether sampling was performed in the control area or in the rill. However, the *S* index differed significantly between the C and B_0 treatments since the former treatment yielded a significantly larger *S* value than the latter one. The relative variability of *S* varied only minimally with the treatment, and it was medium in both cases.

Therefore, rilling did not influence dry soil bulk density. However, as compared with the control, the soil of the rill had a smaller water content at saturation and at −0.1 m, a similar water content at −1 m and a larger water content at −150 m. Consequently, $(\theta_s-\theta_{-0.1m})$ did not vary significantly between the two treatments since both θ_s and $\theta_{-0.1m}$ decreased from the C to the B_0 treatment. A decrease of $(\theta_{-0.1m}-\theta_{-1m})$ occurred in the rilled soil because $\theta_{-0.1m}$ decreased while θ_{-1m} did not vary. The decrease of $(\theta_{-1m}-\theta_{-150m})$ from the C to the B_0 treatment was due to the circumstance that the soil of the rill had a higher θ_{-150m} value than the control. As compared with the non-rilled soil, rilling implied that the volume of pores with $d>300\,\mu m$ did not change. There were fewer pores of both $30\leq d\leq 300\,\mu m$ and $0.2\leq d\leq 30\,\mu m$ and more pores with $d<0.2\,\mu m$. According to the *S* calculations, rilling determined a decrease in the SPQ that, however, remained very good.

The ratio between θ_s and the soil porosity, obtained from ρ_b and assuming a soil particle density of $2.65\,g\,cm^{-3}$, was equal to 1.04

TABLE 1 | Summary statistics of the ρ_b, θ_s, $\theta_{-0.1m}$, θ_{-1m}, θ_{-150m}, θ_s-$\theta_{-0.1m}$, $\theta_{-0.1m}$-θ_{-1m}, θ_{-1m}-θ_{-150m} and S values obtained in the non-rilled upper area of the plot (control, C) and in the rills treated with biochar at a rate of 0% (B_0), 3% (B_3) and 5% (B_5) (sample size, $N=8$ for the C treatment and $N=9$ for the B_0, B_3 and B_5 treatments; d = pore diameter).

Parameter	Statistic	C	B0	B3	B5
ρ_b (g/cm^3)	Min	1.134	1.127	0.920	0.989
	Max	1.298	1.295	1.214	1.186
	Mean	1.235 a	1.207 a A	1.087 B	1.088 B
	CV (%)	4.3	4.7	9.3	6.9
θ_s (m^3/m^3)	Min	0.482	0.429	0.452	0.489
	Max	0.660	0.528	0.597	0.633
	Mean	0.557 a	0.484 b A	0.503 A	0.561 B
	CV (%)	12.8	7.0	10.4	8.8
$\theta_{-0.1m}$ (m^3/m^3) $d \leq 300\,\mu$m	Min	0.412	0.341	0.347	0.393
	Max	0.536	0.448	0.475	0.470
	Mean	0.463 a	0.396 b A	0.412 A	0.449 B
	CV (%)	8.8	8.4	9.6	5.5
θ_{-1m} (m^3/m^3) $d \leq 30\,\mu$m	Min	0.229	0.233	0.218	0.241
	Max	0.260	0.269	0.272	0.305
	Mean	0.248 a	0.249 a A	0.248 A	0.274 B
	CV (%)	4.6	5.7	7.1	7.4
θ_{-150m} (m^3/m^3) $d \leq 0.2\,\mu$m	Min	0.098	0.109	0.098	0.090
	Max	0.109	0.126	0.122	0.114
	Mean	0.103 a	0.117 b A	0.112 A	0.102 B
	CV (%)	3.4	5.0	7.4	7.7
$\theta_s - \theta_{-0.1m}$ (m^3/m^3) $d > 300\,\mu$m; macroporosity	Min	0.052	0.062	0.047	0.054
	Max	0.184	0.115	0.141	0.184
	Mean	0.094 a	0.088 a A	0.091 A	0.112 A
	CV (%)	53.2	21.5	31.0	39.3
$\theta_{-0.1m} - \theta_{-1m}$ (m^3/m^3) $30 \leq d \leq 300\,\mu$m; soil aeration in the soil matrix domain or drainable porosity	Min	0.183	0.108	0.129	0.152
	Max	0.281	0.189	0.203	0.188
	Mean	0.215 a	0.147 b A	0.164 AB	0.175 B
	CV (%)	16.1	17.1	14.2	6.5
$\theta_{-1m} - \theta_{-150m}$ (m^3/m^3) $0.2 \leq d \leq 30\,\mu$m; plant available water capacity	Min	0.131	0.120	0.120	0.151
	Max	0.155	0.144	0.150	0.191
	Mean	0.144 a	0.132 b A	0.136 A	0.172 B
	CV (%)	5.9	6.8	7.9	8.5
S	Min	0.067	0.045	0.066	0.069
	Max	0.103	0.074	0.084	0.094
	Mean	0.083 a	0.058 b A	0.074 B	0.079 B
	CV (%)	16.1	16.8	9.3	10.3

Note: A comparison was established between the C and B_0 treatments using an F test and a two-tailed t test at $p=0.05$. For a given parameter, means followed by the same lower case letter are not significantly different. Means followed by a different lower case letter are significantly different. A pairwise comparison was established between the B_0, B3 and B5 treatments using an F test and a two-tailed t test at $p=0.05$. For a given parameter, means followed by the same upper case letter are not significantly different. Means followed by a different upper case letter are significantly different.

for the C treatment and 0.89 for the B_0 one. Despite the numerical uncertainty linked to a ratio > 1, likely attributable to the approximations of the experiment, the sign was that soil saturation was more complete in the former soil than the latter one. Therefore, shaping the rill and allowing water to move in this incision did not induce soil compaction in the zone surrounding the channel, probably because the rill was formed by gently excavating and removing soil. However, the repeated passage of water promoted some soil alteration with different mechanisms, such as slaking at the beginning of the experiment or weakening of the bonds between soil particles due to wetting or mechanical solicitations (e.g., Le Bissonnais 1996). A part of the smallest and most mobile particles penetrated the soil. These particles did not modify the largest pores since they were too small as compared with these pores. However, they partially occluded pores of intermediate sizes and induced the formation of very small pores.

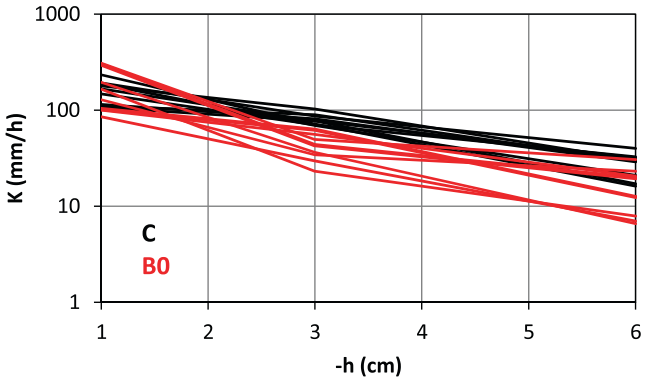

FIGURE 4 | Hydraulic conductivity, K, versus pressure head, h, relationships determined in the non-rilled plot area (C) and the non-treated rill (B_0).

According to the guidelines by Reynolds et al. (2002, 2009), macroporosity and soil aeration in the soil matrix domain were good, but the plant-available water capacity was limited regardless of the treatment. Therefore, the formation of the rill and the establishment of a flow through the incision did not have appreciable effects on the soil's ability to quickly drain excess water and facilitate root proliferation. However, the soil became less aerated in the soil matrix domain and also less able to retain available water for crop growth.

An overlap of the hydraulic conductivity curves obtained with the C and B_0 treatments was noticed close to saturation (Figure 4). For smaller (more negative) pressure heads, the curves obtained in the C area tended to stay above those obtained in the B_0 rill, particularly with reference to the intermediate pressure head established experimentally ($h = -3$ cm). The means of K_{-1cm} did not differ significantly between the two treatments (160–173 mm/h) while the K_{-3cm} and K_{-6cm} values obtained in the B_0 rill were smaller by 1.9 and 1.7 times, respectively, than those obtained in the C zone (Table 2). Regardless of h, the relative variability of the data were more appreciable in the rill than in the non-rilled area. In particular, the coefficients of variation, CV, of K denoted consistently a medium variation in the C area, but they signalled a high variation for two of the three established pressure heads in the B_0 rill (Warrick 1998). In summary, shaping the rill and flow establishment in this rill (i) did not influence hydraulic conductivity of the nearly saturated soil ($h = -1$ cm), (ii) determined a significant decrease of the soil ability to transmit water in more unsaturated conditions ($h \leq -3$ cm) and (iii) enhanced spatial variability of K regardless of the considered pressure head.

Soil erosion can be expected to induce changes in the hydraulic properties of the exposed soil surface (Li et al. 2021).

TABLE 2 | Summary statistics of the soil hydraulic conductivity, K (mm/h), values for different pressure heads, h_0, established in the non-rilled upper area of the plot (control, C) and in the rills treated with biochar at a rate of 0% (B_0), 3% (B_3) and 5% (B_5) (sample size, $N = 8$ for the B_0 treatment and $N = 9$ for the C, B_3 and B_5 treatments).

h_0 (cm)	Statistic	C	B_0	B_3	B_5
−6 $d \leq 0.5$ mm	Min	16.2	6.6	8.6	16.2
	Max	40.0	30.6	39.3	29.5
	Mean	27.5 a	16.0 b A	20.9 AB	24.0 B
	CV (%)	28.6	55.1	46.7	20.1
−3 $d \leq 1$ mm	Min	69.1	23.2	17.6	46.5
	Max	102.6	62.7	99.7	97.8
	Mean	80.6 a	41.9 b A	62.3 B	71.3 B
	CV (%)	13.5	32.3	37.4	27.2
−1 $d \leq 3$ mm	Min	106.5	85.0	119.5	129.6
	Max	234.1	309.1	306.3	560.0
	Mean	159.9 a	173.1 a A	214.3 A	277.7 A
	CV (%)	27.2	51.1	29.7	50.0

Note: A comparison was established between the C and B0 treatments using an F test and a two-tailed t test at $p = 0.05$. For a given pressure head, means followed by the same lower-case letter are not significantly different. Means followed by a different lower-case letter are significantly different. A pairwise comparison was established between the B0, B3 and B5 treatments using an F test and a two-tailed t test at $p = 0.05$. For a given pressure head, means followed by the same upper-case letter are not significantly different. Means followed by a different upper-case letter are significantly different.

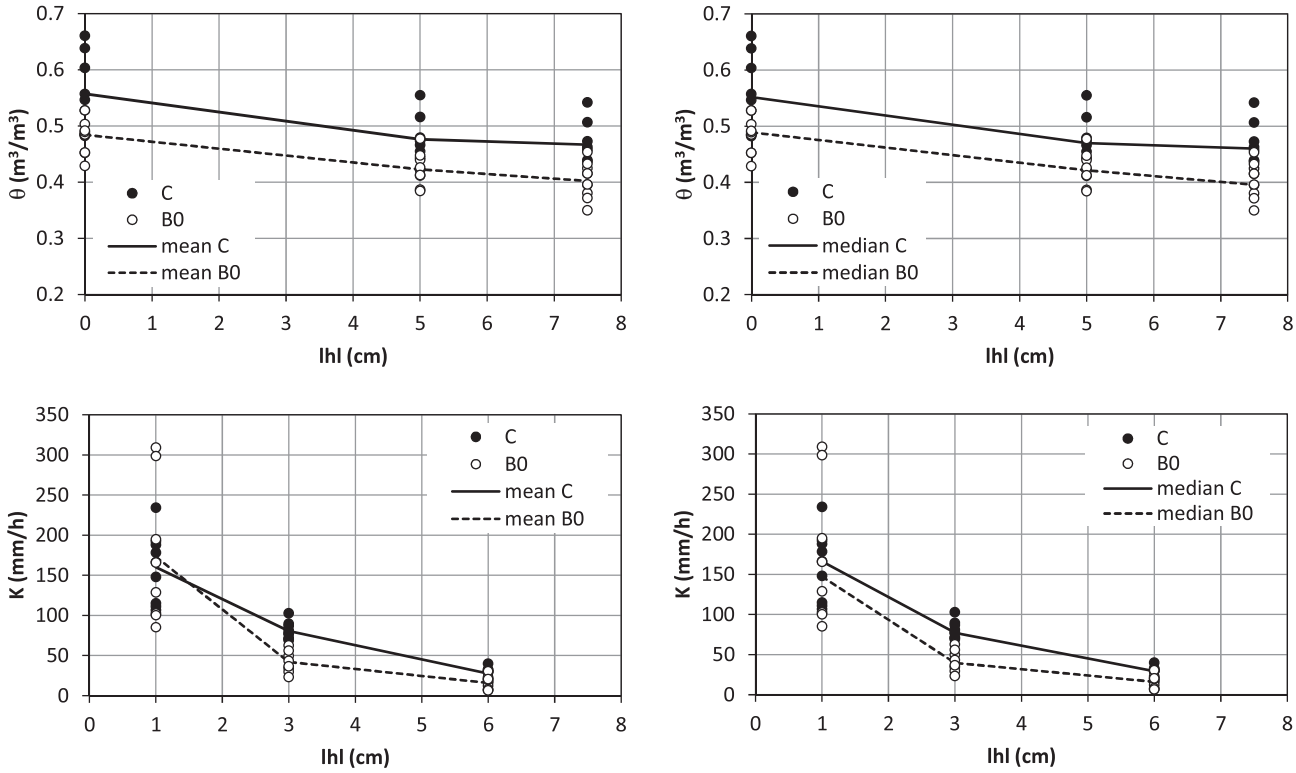

FIGURE 5 | Volumetric soil water content, θ, and soil hydraulic conductivity, K, against the absolute value of the soil water pressure head, h, for the control (C) and the rilled (B_0) soil.

This investigation supported this expectation and also demonstrated that, with reference to the near-saturated soil hydraulic conductivity (close to zero h values), soil erosion effects can change with the considered pressure head. The smaller the imposed pressure head at the soil surface, the smaller the active soil pores in the soil water transport process. Likely, shaping the rill induced some smearing and compaction of the exposed soil surface, and hence a general decrease of K, but soil particle detachment induced by rill flow determined a reactivation of the largest pores. Another, not necessarily alternative, interpretation could be that some of the transported sediments were trapped at the bottom of the rill as a consequence, for example, of surface soil roughness. According to this investigation, these trapped sediments were particularly effective in occluding the smaller exposed pores.

Figure 5 establishes a comparison between the water retention and the hydraulic conductivity relationships obtained under the C and B_0 treatments in the nearly common pressure head range. The figure is repeated twice since the individual data were summarised by both the mean and the median, and reporting all curves on a single plot was found to make some confusion. At least with reference to the medians, there was consistency between the water retention and hydraulic conductivity curves, given that, notoriously, K decreases for smaller θ values. In particular, for high (little negative) pressure heads, rilling induced a decrease in the soil's ability to retain water, and therefore the soil became less conductive. A consistency between water retention and hydraulic conductivity curves was also perceived considering the means, even if, in this case, the results were a little less clear ($h = -1$ cm: C soil was wetter than the B_0 soil but had similar K values).

3.2 | Biochar Addition

Numerically, ρ_b and θ_{-150m} decreased monotonically or almost monotonically in the passage from the B_0 to B_5 treatment. Instead, θ_s, $\theta_{-0.1m}$, θ_{-1m}, $(\theta_s - \theta_{-0.1m})$, $(\theta_{-0.1m} - \theta_{-1m})$ and $(\theta_{-1m} - \theta_{-150m})$ increased more or less monotonically between the two extreme treatments (Table 1). Regardless of the treatment, data variability was low for ρ_b, θ_s, $\theta_{-0.1m}$, θ_{-1m}, θ_{-150m} and $(\theta_{-1m} - \theta_{-150m})$ and medium for $(\theta_s - \theta_{-0.1m})$. The variability of the $(\theta_{-0.1m} - \theta_{-1m})$ values was medium for the B0 treatment and low for the B_3 and B_5 treatments.

The ρ_b values for the B_3 and B_5 treatments were statistically similar and smaller than those obtained with the B_0 treatment. The means of θ_s, $\theta_{-0.1m}$, θ_{-1m} and θ_{-150m} did not differ between the B_0 and B_3 treatments. The B_5 treatment yielded higher θ_s, $\theta_{-0.1m}$ and θ_{-1m} values and smaller θ_{-150m} values than the other two treatments. Macroporosity $(\theta_s - \theta_{-0.1m})$ did not change significantly with the treatment. Soil aeration in the soil matrix domain $(\theta_{-0.1m} - \theta_{-1m})$ varied according to the $B_5 = B_3 \geq B_0$ sequence. The plant available water capacity $(\theta_{-1m} - \theta_{-150m})$ did not differ between the B_0 and B_3 treatments, but it was higher with the B_5 treatment.

The SPQ was very good ($S > 0.05$) regardless of the treatment. However, the B_3 and B_5 treatments yielded statistically similar S values and both these values were significantly higher than that obtained for the B_0 treatment. Adding biochar reduced the variability of S since it was medium for the B_0 treatment and low for both the B_3 and B_5 treatments.

The ratio between θ_s and the soil porosity was not calculated in this case since the assumption that soil particle density was equal to 2.65 g cm^{-3} could not be made due to the presence of biochar.

Therefore, a small amount of biochar (B_3 treatment) was enough to induce a significant decrease in ρ_b that did not decrease further with more biochar (B_5 treatment). Except for θ_{-150m}, the same small amount of biochar tended to generally give larger θ values and θ differences, but not enough to make differences with the untreated soil statistically significant. Instead, these differences became significant with more biochar. With reference to θ_{-150m}, even a small amount of biochar yielded a little smaller value as compared with the non-treated soil, but a large amount of biochar was necessary to make the differences significant.

In summary, as compared with the non-treated soil, a small addition of biochar (3%) did not significantly affect θ_s, $\theta_{-0.1m}$, θ_{-1m} and θ_{-150m}. When more biochar (5%) was used, the first three parameters significantly increased, while the fourth parameter significantly decreased. Consequently, $(\theta_s - \theta_{-0.1m})$ did not change significantly between the B_0 and B_5 treatments since both θ_s and $\theta_{-0.1m}$ increased. An increase of $(\theta_{-0.1m} - \theta_{-1m})$ occurred because $\theta_{-0.1m}$ increased more (by $0.053\,m^3\,m^{-3}$) than θ_{-1m} (by $0.025\,m^3\,m^{-3}$). Finally, $(\theta_{-1m} - \theta_{-150m})$ increased because θ_{-1m} increased and θ_{-150m} decreased. As compared with the non-treated soil, adding 5% of biochar implied that the volume of pores with $d > 300\,\mu m$ did not change. There were more pores of both $30 \le d \le 300\,\mu m$ and of $0.2 \le d \le 30\,\mu m$ and less pores with $d \le 0.2\,\mu m$. According to guidelines by Reynolds et al. (2002, 2009), macroporosity and soil aeration in the soil matrix domain were good regardless of the treatment. Instead, the plant-available water capacity was limited for the B_0 and B_3 treatments and good for the B_5 treatment.

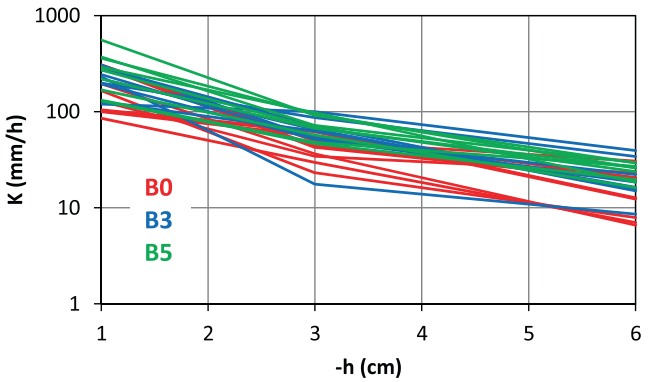

FIGURE 6 | Hydraulic conductivity, K, versus pressure head, h, relationships determined in the non-treated rill (B_0) and in the treated rills with biochar at a rate of 3% (B_3) and 5% (B_5).

According to the S calculations, even a relatively small addition of biochar (B_3 treatment) was enough to significantly improve the SPQ. With more biochar (B_5 treatment), the differences between the treated and non-treated soils became larger. However, the two treatments with biochar did not differ significantly, suggesting that using 5% of biochar instead of 3% had a limited effect on S. Adding biochar made S calculations less variable, suggesting a homogenising effect of the treatment, even for a relatively small percentage of biochar.

A partial overlap of the hydraulic conductivity curves obtained with the B_0, B_3 and B_5 treatments was noticed close to saturation (Figure 6). For more negative pressure heads, the curves obtained in the B_3 and B_5 rills appeared to overlap with each other and overall stay above those obtained in the B_0 rill. For all established pressure heads, K increased monotonically with the applied amount of biochar. In particular, K for the B_5 rill was 1.5–1.7 times greater than K for the B_0 rill, depending on h.

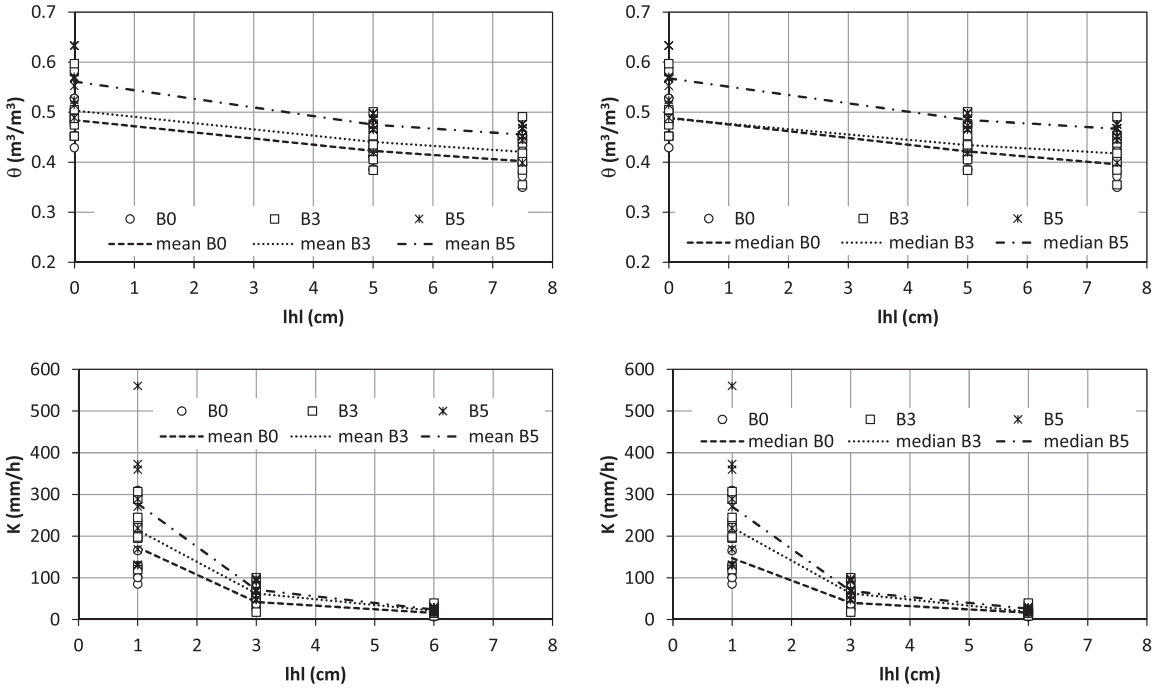

FIGURE 7 | Volumetric soil water content, θ and soil hydraulic conductivity, K, against the absolute value of the soil water pressure head, h, for the rilled soil with different concentrations of biochar (0%: B_0; 3%: B_3; 5%: B_5).

The means of K_{-1cm} did not differ significantly among the three treatments (173–278 mm h^{-1}; Table 2). Those of K_{-3cm} varied between 42 and 71 mm/h according to the $B_5 = B_3 > B_0$ sequence. Finally, the means of K_{-6cm} varied between 16 and 24 mm h^{-1} according to the $B_5 = B_3 \geq B_0$ sequence. Relative variability of K decreased monotonically from the B_0 to the B_5 rill with reference

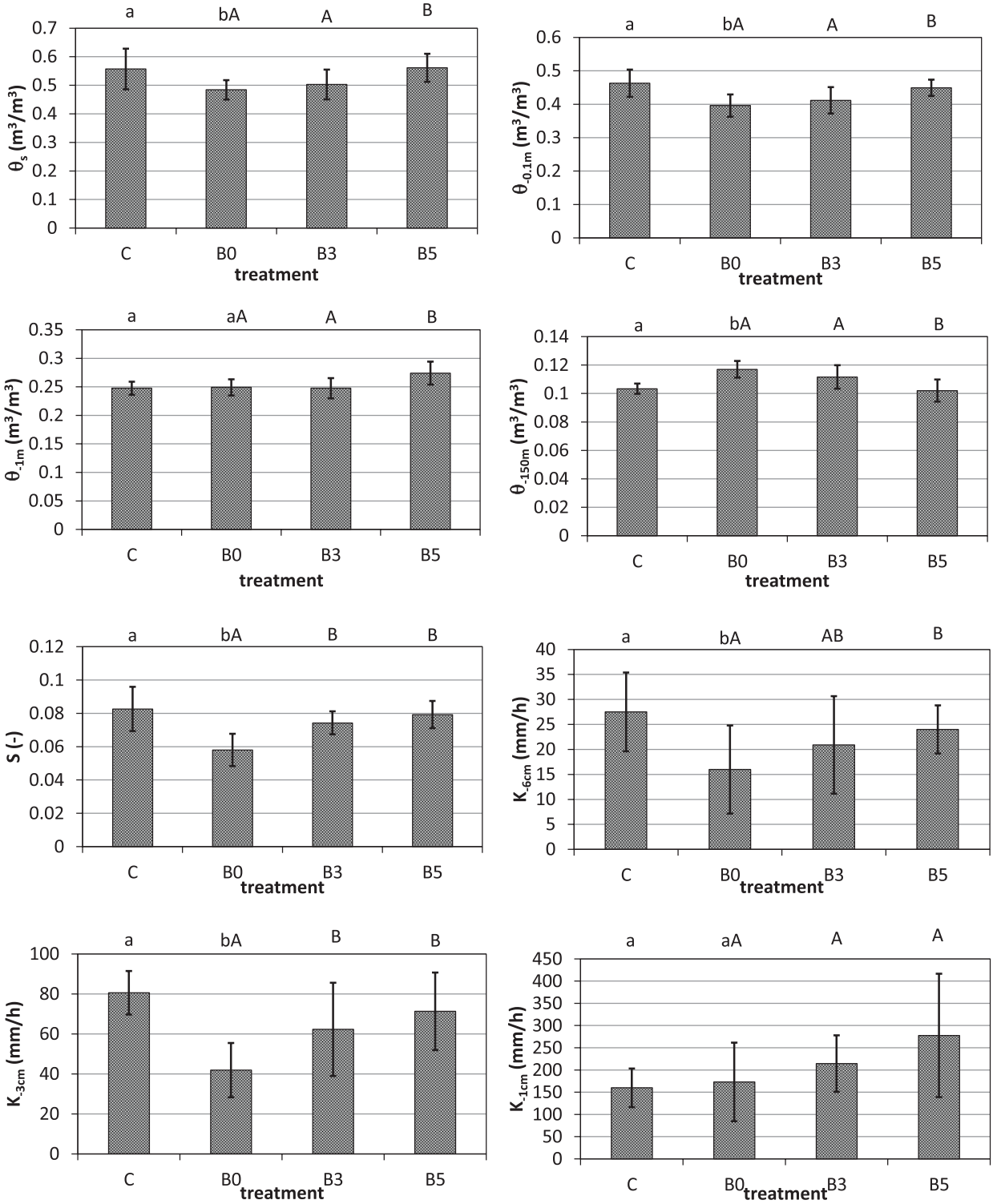

FIGURE 8 | Means of saturated soil volumetric water content, θ_s, volumetric soil water content at a pressure head of −0.1 m ($\theta_{-0.1m}$), −1 m (θ_{-1m}), −150 m (θ_{-150m}), *S*-index and soil hydraulic conductivity at a pressure head value of −6 cm (K_{-6cm}), −3 cm (K_{-3cm}) and −1 cm (K_{-1cm}) for four soil treatments (C: control; B_0: rilled soil; B_3: Rilled soil with 3% of biochar; B_5: Rilled soil with 5% of biochar). Error bars represent ± one standard deviation. Histograms denoted by the same lower (comparison between the C and B0 treatments) or upper (comparison between the B_0, B_3 and B_5 treatments) case letters indicate that means did not differ significantly at $p = 0.05$. Histograms denoted by different lower- or upper-case letters indicate that means differed significantly.

to K_{-6cm}, but a similar trend was not detected for the other two pressure heads since the B_3 rill yielded the highest *CV* with reference to K_{-3cm} and the lowest *CV* of K_{-1cm}.

Therefore, regardless of h, using 3% or 5% of biochar did not induce statistically significant differences between the corresponding K values. For the highest pressure head ($h = -1$ cm), adding biochar did not significantly modify the soil hydraulic conductivity. For the intermediate pressure head ($h = -3$ cm), even a limited concentration of biochar (3%) determined a significant increase in K. For the most negative pressure head ($h = -6$ cm), a significant increase in K as compared with a non-treated soil (B_0) required adding 5% of biochar. In other terms, from a purely numerical point of view, the inclusion of biochar in the soil improved, in general, the soil aptitude to transmit water, regardless of the pore size. This improvement was statistically irrelevant in the case of a transport process governed by the larger pores. Instead, the water transport ability of the smallest pores ($h \leq -3$ cm) increased with a high percentage of biochar.

A variety of results have been reported for other loamy soils, texturally similar, in a broad sense, to the one considered in this investigation. According to Blanco-Canqui (2017), the addition of biochar can be expected to reduce unsaturated conductivity close to saturation due to the filling or clogging of soil macropores with fine biochar particles. An increase in near-saturated conductivity in biochar-amended soils can instead occur as a consequence of increased earthworm burrowing (Hardie et al. 2014). Biochar may enhance the transport of water under unsaturated conditions by reducing the formation of larger pores (draining pores) and promoting finer inter-particle pore formation (Villagra-Mendoza and Horn 2018). The results of this investigation were not consistent with the suggestion by Blanco-Canqui (2017), nor were explained by earthworm activity since earthworms were not noticed, and in any case, the experiments were performed after a short incubation period. Instead, the suggestion by Villagra-Mendoza and Horn (2018) appeared approximately adaptable to our data. In particular, biochar addition was statistically ineffective with reference to the largest sampled pores, but including a relatively high amount of this amendment (5%) favoured the formation of smaller pores, that is, those active for pressure heads smaller than or equal to −3 cm.

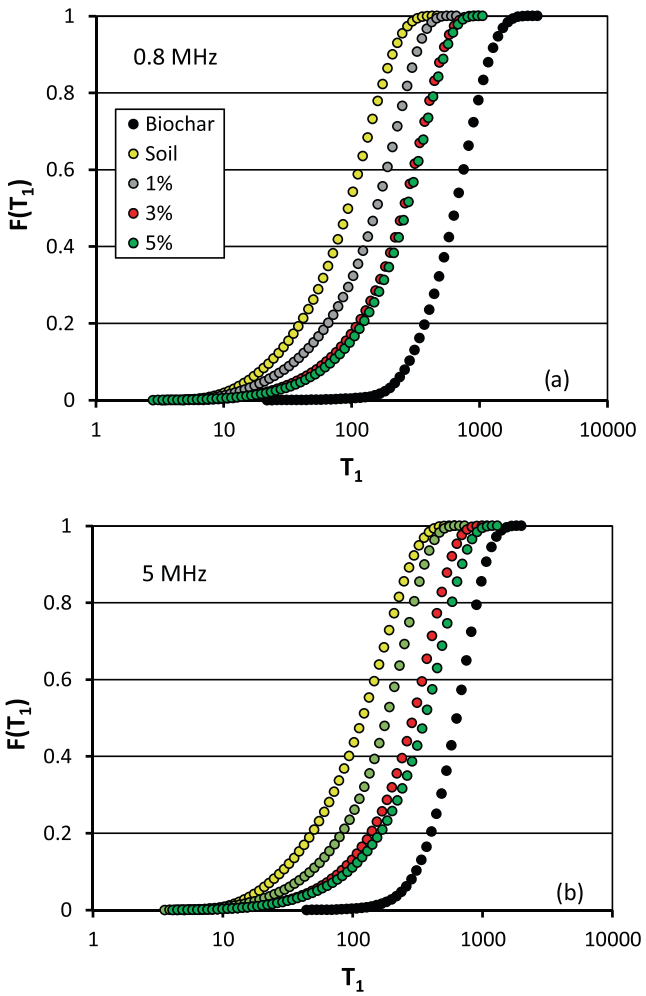

FIGURE 9 | Empirical cumulative frequency distributions $F(T_1)$ of the investigated samples (Biochar, C, B_1, B_3 and B_5) for two applied proton Larmor frequencies.

Another way to summarise the results is to recognise that there is some correspondence between the static porosity, as determined from the water retention measurements, and the dynamic porosity determined by the UHG experiment. Macroporosity does not change but the drainable porosity increases. Taking into account that K is an integral measurement, expressive of flow in all porosity classes from zero to the upper boundary, it is plausible to believe that, for $h = -6$ cm, the weight of the drainable porosity is greater and this explains the increase of K_{-6}. For $h = -1$ cm, the contribution of the macroporosity prevails and for this reason significant differences in K_{-1} are not detected even if the mean increases anyway.

Figure 7 establishes a comparison between the water retention and the hydraulic conductivity relationships corresponding to the B_0, B_3 and B_5 treatments in a common range of high pressure head values. Also in this case, the figure is repeated twice since the individual data were summarised by both the mean and the median. Considering the means, the water retention and hydraulic conductivity curves appeared consistent between them since adding biochar increased the soil's ability to retain water and hence its ability to transmit water. A consistency between water retention and hydraulic conductivity curves was also perceived considering the medians, even if, in this case, the results were a little less clear ($h = -1$ cm: similar θ value for the B_0 and B_3 soils but a higher K value in the treated soil).

3.3 | Combined Rilling and Biochar Addition Effects

Figure 8 compares the means of θ_s, $\theta_{-0.1m}$, θ_{-1m}, θ_{-150m}, S, K_{-6cm}, K_{-3cm} and K_{-1cm} for the four treatments considered in this investigation (C, B_0, B_3, B_5).

Rilling of the non-treated soil (B_0) determined a decrease of θ_s, $\theta_{-0.1m}$, S, K_{-6cm} and K_{-3cm} and an increase of θ_{-150m} as compared with the control (C). The addition in the rill of a relatively large amount of biochar (B_5) effectively contrasted these rilling effects since θ_s, $\theta_{-0.1m}$, θ_{-150m}, S, K_{-6cm} and K_{-3cm} did not appear to differ appreciably between the C and B_5 treatments. Rilling effects were

also contrasted by adding a relatively small amount of biochar (B_3), but to a more limited extent. Neither rilling alone nor rilling in a soil with a relatively low biochar content (B_3) resulted in appreciable variations in θ_{-1m} compared to the control. Instead, adding relatively high amounts of biochar in the rilled soil (B_5) yielded higher θ_{-1m} values both with respect to the control and with reference to the other two rills (B_0, B_3). Finally, rilling (B_0) did not appear to appreciably alter K_{-1cm} as compared with the control. However, more biochar in the rill implied obtaining higher K_{-1cm} values.

Therefore, six (θ_s, $\theta_{-0.1m}$, θ_{-150m}, S, K_{-6cm} and K_{-3cm}) of the eight considered parameters consistently indicated that (i) in the absence of any treatment with biochar, rilling altered the soil characteristics, and (ii) the addition of a large amount of biochar impeded these alterations to occur. In other terms, the changes induced by rilling were compensated by the presence of biochar in the soil. This interpretation is not contradicted by the results obtained with the other two parameters (θ_{-1m} and K_{-1cm}), since in this case the suggestion was that the addition of large amounts of biochar in the rill can make the soil even more able than the non-rilled soil to retain water at field capacity and more conductive in close to saturation conditions.

3.4 | NMR Measurements on Soil Samples With Different Biochar Concentration

For calculating *FCI* and *SCI* indexes, the empirical cumulative frequency distributions of the longitudinal relaxation time ($F(T_1)$ distribution) for the relaxograms corresponding to the B_1, B_3, B_5 and C treatments, and the applied biochar measured at the different applied magnetic fields were examined. Figure 9 shows, as an example for two values of the applied magnetic field (ν_L of 0.8 and 5 MHz), the detected $F(T_1)$ distribution. For each ν_L value, the relaxation time distribution of the investigated soil (C treatment) is always on the left of the $F(T_1)$ corresponding to the other treatments. Therefore, the shortest T_1 values correspond to the soil, while, on the contrary, biochar is characterised by the longest T_1 values. This detected difference between the original soil and the three

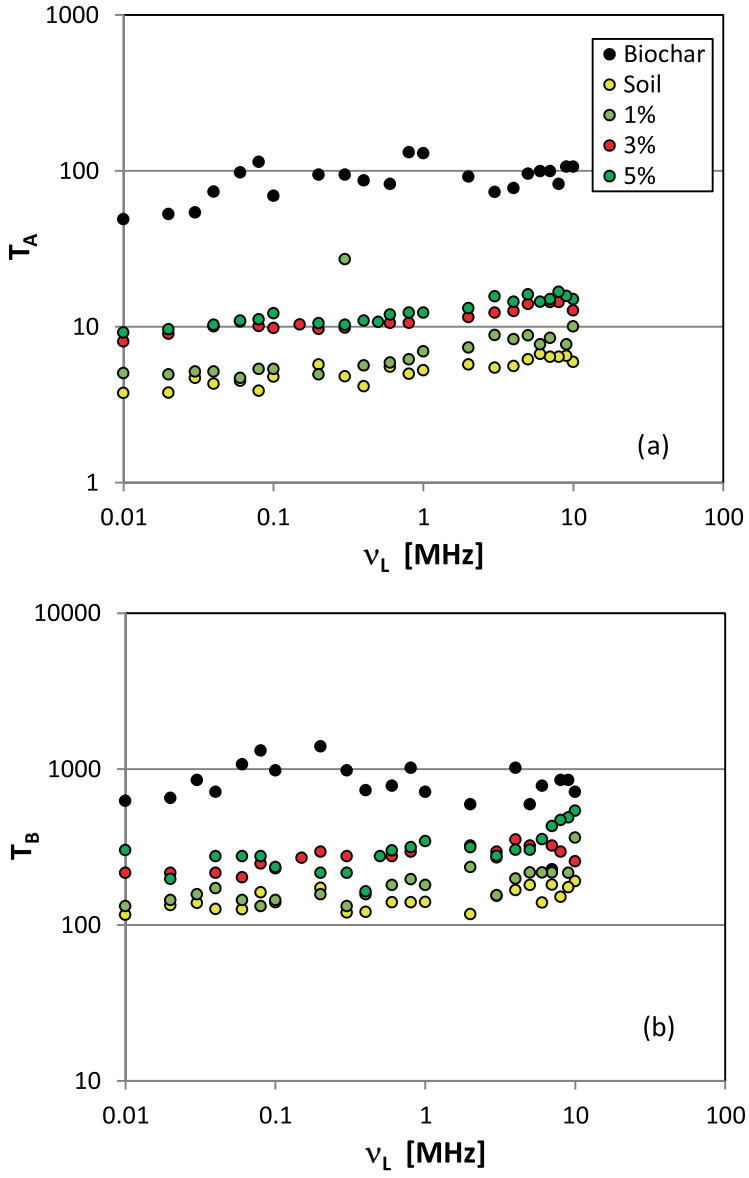

FIGURE 10 | Relationship between the applied proton Larmor frequency ν_L and T_A (a) and T_B (b) for all the investigated samples.

mixtures of soil and biochar (i.e., B_1, B_3 and B_5 treatments) can be attributed to the increase in size of the pores in the latter due to the biochar component. Figure 9 also highlights that all $F(T_1)$ distributions are S-shaped and skewed towards shorter T_1 values, suggesting that the macro-pore component (largest T_1 values) is not dominant, and the biochar addition increases the size of mesopores and micropores. The overlapping between the $F(T_1)$ distributions corresponding to BC = 3 and 5% establishes that this increase does not produce appreciable changes in the pore distribution inside the mixture.

For a given percentage of biochar, Figure 10 shows the variation of T_A, which is indicative of water molecules contained in small pores, and T_B, corresponding to water contained in large pores, with the proton Larmor frequency ν_L. Figure 10 points out that (i) the highest T_A and T_B values are characteristic of soil-biochar mixtures, while the lowest values correspond to the soil; (ii) T_A and T_B are independent of ν_L; (iii) T_A and T_B increase with the biochar percentage. Furthermore, Figure 10 demonstrates that B_3 and B_5 treatments are characterised by similar values of T_A and T_B. In other words, a biochar amount equal to 5% can be considered a limit value to obtain appreciable variations of the micro-pores and macro-pores as compared to the original soil. From a hydrological point of view, the increase of *BC* from 3% to 5% does not change the micro-pore and the macro-pore components. This result agrees with those obtained by Li et al. (2019, 2020) and Gholamahmadi et al. (2023), who found a threshold value of biochar addition effectiveness equal to 3% and 2.5%, respectively.

According to a previous study (Conte and Ferro 2020), the *SCI* and *FCI* values of the investigated mixtures measured applying different magnetic fields were merged into a single statistical sample, thereby obtaining the corresponding cumulative frequency distributions plotted in Figure 11. For each index, Figure 11 shows that the empirical cumulative frequency distribution of the biochar is always placed on the left-hand side of that of the original soil, that is, the *SCI* and *FCI* values for the soil sample are always greater than those of the biochar. Figure 11a also demonstrates that the B_5 treatment has higher *SCI* values than B_1 and B_3, for which, instead, the index distributions overlap. Figure 11b points out that *FCI* distributions for C and B_1 treatments overlap as well as those for the B_3 and B_5 ones, and the latter shift to the left as compared to the former. This result reveals that, with respect to the original soil, *FCI* does not reduce further beyond *BC* = 3% Therefore, biochar concentrations of 5% and 3% are discriminating values for *SCI* and *FCI*, respectively.

In conclusion, the developed analysis demonstrated that the FFC NMR technique is able to measure the two components, *SCI* and *FCI*, of the HCS and their variability with the percentage of biochar added to the original soil.

3.5 | Combination of Hydrological and NMR Measurements

One of the innovative aspects of this investigation was the attempt to look at the pore system from two different observation scales: a macroscopic scale by the hydrological measurements and a microscopic or molecular scale by the NMR measurements. In both cases, the pore size distribution, leading to categorization into macropores, mesopores and micropores, was estimated and not measured directly. In particular, hydrological data were analysed by the Young-Laplace equation under the assumption that the pores are perfectly cylindrical, uniform and equally drained (e.g., Hardie et al. 2014). For the NMR data, the correspondence between pore sizes and the measured relaxogram represented an assumption (Conte and Ferro 2018) still needing testing. A comparison between the hydrological and the NMR data were made to verify if there was a link between the two approaches.

The water volume contained in the macropores ($d > 300\,\mu m$) did not change significantly between the non-treated rilled soil (B_0 treatment) and the rilled soil treated with 5% of biochar (B_5 treatment) (Table 1). However, the FFC NMR investigations revealed that the size of the largest pores ($d \geq 50\,\mu m$) increased as comparing the untreated soil and the biochar/soil mixture (Figure 9). By considering the hydrological and NMR measurements together, it is possible to suggest that the former investigation can be affected by the larger pore-size scale ($d > 300\,\mu m$) in comparison with the NMR analysis ($d \geq 50\,\mu m$). As a consequence, the amount of free bulk water affecting the hydrological measurements is larger than that present during the NMR investigations. Moreover, the

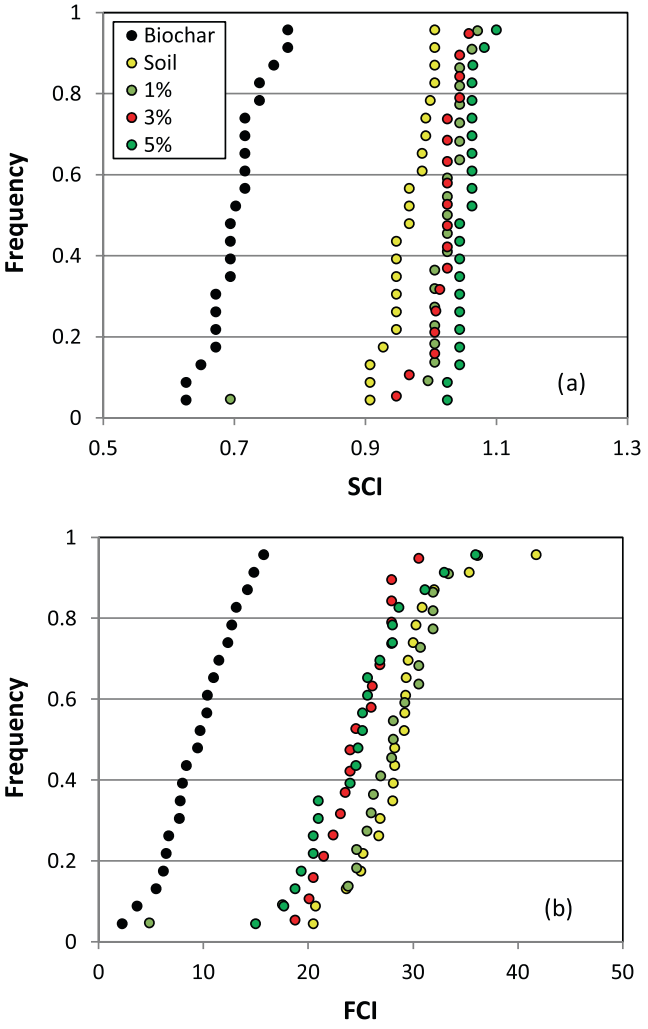

FIGURE 11 | Empirical frequency distributions of SCI (a) and FCI (b) for all the investigated samples.

combined results appear to suggest that while the total volume of the largest pores remains constant, the number of pores can decrease. In other words, the addition of biochar did not alter total pore volume but could modify only the total number of pores, determining fewer macropores having larger sizes.

Adding biochar increased the water volume contained in pores of intermediate size ($0.2 \leq d \leq 300\,\mu m$), and the NMR analysis signalled an increase in the size of the mesopores. In this case, it was not possible to draw a conclusion on the number of mesopores since three different combinations (larger and more numerous mesopores, larger but unvaried number of mesopores and larger but fewer mesopores) can be expected to yield the result that was obtained with the water retention measurements.

Finally, less water was contained in the micropores of $< 0.2\,\mu m$, but the NMR data suggested an increase in the size of these pores with the addition of biochar. Therefore, the suggestion was that in the treated soil there were fewer small pores, but they were greater than those in the non-treated soil.

The scale difference and the uncertainties in the analysis methodologies of the data that are actually collected (soil water content for established pressure heads with the hydrological measurements and relaxogram for the NMR measurements) induce not to exclude that the two types of measurement may be disconnected from each other. However, it cannot even be ruled out that there is some link between the two experimental approaches since soil-water interactions are investigated in both cases. According to the results of this investigation, the latter hypothesis appears to have some support. Consequently, additional efforts should be made to develop a clear relationship between the two different types of measurements.

4 | Conclusions

Contrasting effects of biochar addition on runoff and soil loss have been reported in the literature, and the existence of a threshold value of biochar concentration useful for soil conservation strategies needs further investigations. In this study, the effects of rill formation and biochar addition on the physical and hydraulic properties of a clay-loam soil were assessed by laboratory measurements and field tests.

According to the water retention measurements performed on a clay-loam soil, the formation of the rill and establishment of a flow through the incision can be expected to have no appreciable effect on the soil's ability to quickly drain excess water and facilitate root proliferation. However, the soil could become less aerated in the soil matrix domain and also less able to retain readily available water for crop growth. As compared with a non-treated rilled soil, adding 5% of biochar to the soil surrounding the rill incision can imply that the volume of pores with diameter $d > 300\,\mu m$ does not change. More pores of both $30 \leq d \leq 300\,\mu m$ and of $0.2 \leq d \leq 30\,\mu m$ and fewer pores with $d \leq 0.2\,\mu m$ can develop.

On the basis of the water transmission parameters determined in this investigation, shaping the rill and flow establishment in this rill could not influence the hydraulic conductivity of the nearly saturated soil (pressure head, $h = -1$ cm), but it could also determine a significant decrease in the soil ability to transmit water in more unsaturated conditions ($h \leq -3$ cm). Inclusion of biochar in the soil can be expected to improve, in general, the soil aptitude to transmit water, regardless of the pore size. This improvement could be statistically irrelevant in the case of a transport process governed by the larger pores. Instead, the water transport ability of the smallest pores ($h \leq -3$ cm) can increase with a high percentage of biochar.

The NMR measurements revealed that the increase of *BC* from 3% to 5% does not change the micro- and macro-pore components, and biochar addition of 5% can be considered a limit value to obtain appreciable variations of the micro-pores and macropores as compared to the original soil. Furthermore, the addition of biochar to the original soil improves the structural connectivity component, while the functional connectivity index of the mixtures is similar to that of the original soil only for $BC = 1\%$, it does not change between *BC* contents of 3% and 5% and lowers as compared to the original soil.

Finally, the combination of hydrological and NMR measurements suggested that a relation between the water volume contained in the pores and the NMR results (distribution of T_1, size of the pores) can be established.

In conclusion, the hydrological measurement demonstrated that the addition of biochar to the soil improved, in general, the soil aptitude to transmit water, regardless of the pore size and demonstrated that the addition of a large amount of biochar (5%) impeded soil characteristics alteration as the changes due to rilling were compensating by adding biochar in the soil. NMR measurements revealed that the mixture of soil and biochar was characterised by longitudinal relaxation time T_1 values, which are related to pore sizes, longer than those measured for the soil. The analysis also suggested that the macro-pore component (i.e., the largest T_1 values) was never dominant, while biochar addition increased the size of mesopores and micropores.

Author Contributions

Vincenzo Bagarello: conceptualization, investigation, funding acquisition, writing – original draft, methodology, validation, visualization, writing – review and editing, software, formal analysis, data curation, supervision, resources, project administration. **Pellegrino Conte:** conceptualization, investigation, writing – original draft, methodology, validation, visualization, writing – review and editing, software, formal analysis, data curation, supervision. **Vito Ferro:** conceptualization, investigation, writing – original draft, methodology, validation, visualization, writing – review and editing, software, formal analysis, data curation, supervision. **Massimo Iovino:** conceptualization, investigation, writing – original draft, methodology, validation, visualization, writing – review and editing, software, formal analysis, data curation, supervision. **Calogero Librici:** conceptualization, investigation, writing – original draft, methodology, visualization, writing – review and editing, software, formal analysis, data curation. **Alessio Nicosia:** conceptualization, investigation, writing – original draft, methodology, validation, visualization, writing – review and editing, software, formal analysis, data curation. **Vincenzo Palmeri:** conceptualization, investigation, writing – original draft, methodology, validation, visualization, writing – review and editing, software, formal analysis, data curation. **Vincenzo**

Pampalone: conceptualization, investigation, writing – original draft, methodology, validation, visualization, writing – review and editing, software, formal analysis, data curation. **Francesco Zanna:** conceptualization, investigation, writing – original draft, methodology, visualization, writing – review and editing, formal analysis, software, data curation.

Acknowledgements

All authors set up the research, analysed and interpreted the results and contributed to write the paper. Open access publishing facilitated by Monash University, as part of the Wiley - Monash University agreement via the Council of Australian University Librarians.

Data Availability Statement

The data that support the findings of this study are available from the corresponding author upon reasonable request.

References

Abrol, V., M. Ben-Hur, F. G. A. Verheijen, et al. 2016. "Biochar Effects on Soil Water Infiltration and Erosion Under Seal Formation Conditions: Rainfall Simulation Experiment." *Journal of Soils and Sediments* 16: 2709–2719.

Baartman, J. E. M., R. Masselink, S. D. Keesstra, and A. J. A. M. Temme. 2013. "Linking Landscape Morphological Complexity and Sediment Connectivity." *Earth Surface Processes and Landforms* 38: 1457–1471. https://doi.org/10.1002/esp.3434.

Bagarello, V., M. Castellini, and M. Iovino. 2007. "Comparison of Unconfined and Confined Unsaturated Hydraulic Conductivity." *Geoderma* 137: 394–400.

Bagarello, V., and M. Iovino. 2012. "Testing the BEST Procedure to Estimate the Soil Water Retention Curve." *Geoderma* 187-188: 67–76. https://doi.org/10.1016/j.geoderma.2012.04.006.

Baiamonte, G., C. De Pasquale, V. Marsala, et al. 2015. "Structure Alteration of a Sandy-Clay Soil by Biochar Amendements." *Journal of Soils and Sediments* 15: 816–824.

Belisle, M. 2005. "Measuring Landscape Connectivity: The Challenge of Behavioural Landscape Ecology." *Ecology* 86: 1988–1995.

Blanco-Canqui, H. 2017. "Biochar and Soil Physical Properties." *Soil Science Society of America Journal* 81: 687–711. https://doi.org/10.2136/sssaj2017.01.0017.

Bondì, C., M. Castellini, and M. Iovino. 2022. "Compost Amendment Impact on Soil Physical Quality Estimated From Hysteretic Water Retention Curve." *Watermark* 14: 1002. https://doi.org/10.3390/w14071002.

Borgia, G. C., R. J. S. Brown, and P. Fantazzini. 1998. "Uniform-Penalty Inversion of Multiexponential Decay Data." *Journal of Magnetic Resonance* 132, no. 1: 65–77. https://doi.org/10.1006/jmre.1998.1387.

Borrelli, P., D. A. Robinson, L. R. Fleischer, et al. 2017. "An Assessment of the Global Impact of 21st Century Land Use Change on Soil Erosion." *Nature Communications* 8, no. 1: 1–13.

Bracken, J., and J. Croke. 2007. "The Concept of Hydrological Connectivity and Its Contribution to Understanding Runoff-Dominated Geomorphic Systems." *Hydrological Processes* 21: 1749–1763. https://doi.org/10.1002/hyp.6313.

Bracken, L. J., J. Wainwright, G. A. Ali, et al. 2013. "Concepts of Hydrological Connectivity: Research Approaches, Pathways and Future Agendas." *Earth-Science Reviews* 119: 17–34. https://doi.org/10.1016/j.earscirev.2013.02.001.

Carollo, F. G., C. Di Stefano, A. Nicosia, V. Palmeri, V. Pampalone, and V. Ferro. 2021. "Flow Resistance in Mobile Bed Rills Shaped in Soils With Different Texture." *European Journal of Soil Science* 72: 2062–2075.

Carollo, F. G., C. Di Stefano, A. Nicosia, V. Palmeri, V. Pampalone, and V. Ferro. 2023. "A New Strategy to Assure Compliance With Soil Loss Tolerance at a Regional Scale." *Catena* 223: 106945.

Castellini, M., L. Giglio, M. Niedda, A. D. Palumbo, and D. Ventrella. 2015. "Impact of Biochar Addition on the Physical and Hydraulic Properties of a Clay Soil." *Soil & Tillage Research* 154: 1–13. https://doi.org/10.1016/j.still.2015.06.016.

Chia, W. Y., K. W. Chew, C. F. Le, et al. 2020. "Sustainable Utilization of Biowaste Compost for Renewable Energy and Soil Amendments." *Environmental Pollution* 267: 115662.

Conte, P. 2019. "Environmental Applications of Fast Field-Cycling NMR Relaxometry." In *Field-Cycling NMR Relaxometry: Instrumentation, Model Theories and Applications*, edited by R. Kimmich, 229–254. UK: Royal Society of Chemistry, Croydon CRo 4YY.

Conte, P. 2021. "Applications of Fast Field Cycling NMR Relaxometry Annual Reports in NMR." *Spectroscopy* 104: 141–188.

Conte, P., R. Bertani, P. Sgarbossa, et al. 2021. "Recent Developments in Understanding Biochar's Physical–Chemistry." *Agronomy* 11, no. 4: 615.

Conte, P., C. Di Stefano, V. Ferro, V. A. Laudicina, and E. Palazzolo. 2017. "Assessing Hydrological Connectivity Inside a Soil by Fast-Field-Cycling Nuclear Magnetic Resonance Relaxometry and Its Link to Sediment Delivery Processes." *Environment and Earth Science* 76: 526. https://doi.org/10.1007/s12665-017-6861-9.

Conte, P., and V. Ferro. 2018. "Measuring Hydrological Connectivity Inside a Soil by Low Field Nuclear Magnetic Resonance Relaxometry." *Hydrological Processes* 32: 93–101. https://doi.org/10.1002/hyp.11401.

Conte, P., and V. Ferro. 2020. "Standardizing the Use of Fast-Field Cycling NMR Relaxometry for Measuring Hydrological Connectivity Inside the Soil." *Magnetic Resonance in Chemistry* 58: 41–50. https://doi.org/10.1002/mrc.4907.

Conte, P., and V. Ferro. 2022. "Measuring Hydrological Connectivity Inside Soils With Different Texture by Fast Field Cycling Nuclear Magnetic Resonance Relaxometry." *Catena* 209: 105848. https://doi.org/10.1016/j.catena.2021.105848.

Conte, P., and P. Lo Meo. 2020. "Nuclear Magnetic Resonance With Fast Field-Cycling Setup: A Valid Tool for Soil Quality Investigation." *Agronomy* 10: 1040.

Dane, J. H., and J. W. Hopmans. 2002. "Water Retention and Storage: Laboratory." In *Methods of Soil Analysis, Physical Methods, Part 4*, edited by J. H. Dane and G. C. Topp, 688–692. Madison, WI: Soil Science Society of America.

Dexter, A. R. 2004. "Soil Physical Quality. Part I: Theory, Effects of Soil Texture, Density, and Organic Matter, and Effects on Root Growth." *Geoderma* 120: 201–214.

Dexter, A. R., and E. A. Czyż. 2007. "Applications of S-Theory in the Study of Soil Physical Degradation and Its Consequences." *Land Degradation & Development* 18: 369–381.

Dexter, A. R., E. A. Czyż, G. Richard, and A. Reszkowska. 2008. "A User-Friendly Water Retention Function That Takes Account of the Textural and Structural Pore Spaces in Soil." *Geoderma* 143: 243–253. https://doi.org/10.1016/j.geoderma.2007.11.010.

Di Stefano, C., A. Nicosia, V. Palmeri, V. Pampalone, and V. Ferro. 2022. "Rill Flow Resistance Law Under Sediment Transport." *Journal of Soils and Sediments* 22: 334–347. https://doi.org/10.1007/s11368-021-03083-x.

Doan, T. T., T. Henry-des-Tureaux, C. Rumpel, J. L. Janeau, and P. Jouquet. 2015. "Impact of Compost, Vermicompost and Biochar on Soil Fertility, Maize Yield and Soil Erosion in Northern Vietnam: A Three Year Mesocosm Experiment." *Science of the Total Environment* 514: 147–154.

Dokoohaki, H., F. E. Miguez, D. Laird, R. Horton, and A. S. Basso. 2017. "Assessing the Biochar Effects on Selected Physical Properties of

a Sandy Soil: An Analytical Approach." *Communications in Soil Science and Plant Analysis* 48: 1387–1398. https://doi.org/10.1080/00103624.2017.1358742.

Fouladidorhani, M., M. Shayannejad, M. R. Mosaddeghi, H. Shariatmadari, and E. Arthur. 2023. "Biochar, Manure and Superabsorbent Improve the Physical Quality of Saline-Sodic Soil Under Greenhouse Conditions." *Soil Science Society of America Journal* 87: 1003–1017. https://doi.org/10.1002/saj2.20538.

Gholamahmadi, B., S. Jeffery, O. Gonzales-Pelayo, et al. 2023. "Biochar Impacts on Runoff and Soil Erosion by Water: A Systematic Global Scale Meta-Analysis." *Science of the Total Environment* 871: 161860. https://doi.org/10.1016/j.scitotenv.2023.161860.

Gląb, T., J. Palmowska, T. Zaleski, and K. Gondek. 2016. "Effect of Biochar Application on Soil Hydrological Properties and Physical Quality of Sandy Soil." *Geoderma* 281: 11–20. https://doi.org/10.1016/j.geoderma.2016.06.028.

Hao, X., B. C. Ball, J. L. B. Culley, M. R. Carter, and G. W. Parkin. 2008. "Chapter 57 Soil Density and Porosity." In *Soil Sampling and Methods of Analysis*, edited by M. R. Carter and E. G. Gregorich, 2nd ed., 743–759. Boca Raton, FL: Taylor & Francis Group.

Hardie, M., B. Clothier, S. Bound, G. Oliver, and D. Close. 2014. "Does Biochar Influence Soil Physical Properties and Soil Water Availability?" *Plant and Soil* 376: 347–361. https://doi.org/10.1007/s11104-013-1980-x.

Hseu, Z. Y., S. H. Jien, W. H. Chien, and R. C. Liou. 2014. "Impacts of Biochar on Physical Properties and Erosion Potential of a Mudstone Slopeland Soil." *Scientific World Journal* 2014: 602197.

Jarvis, N. J., L. Zavattaro, K. Rajkai, et al. 2002. "Indirect Estimation of Near-Saturated Hydraulic Conductivity From Readily Available Soil Information." *Geoderma* 108: 1–17.

Jien, S. H., and C. S. Wang. 2013. "Effects of Biochar on Soil Properties and Erosion Potential in a Highly Weathered Soil." *Catena* 110: 225–233.

Keesstra, S. S., V. Bagarello, V. Ferro, D. Finger, and A. J. Parsons. 2020. "Connectivity in Hydrology and Sediment Dynamics." *Land Degradation and Development* 31: 2525–2528. https://doi.org/10.1002/ldr.3401.

Klute, A., and C. Dirksen. 1986. "Hydraulic Conductivity and Diffusivity: Laboratory Methods." *Methods of Soil Analysis: Part 1 Physical and Mineralogical Methods* 5: 687–734.

Köppen, W. 1918. "Classification of Climates According to Temperature, Precipitation and Seasonal Cycle." *Petermanns Geographische Mitteilungen* 64: 193–203.

Kroetsch, D., and C. Wang. 2008. "Chapter 55 Particle Size Distribution." In *Soil Sampling and Methods of Analysis*, edited by M. R. Carter and E. G. Gregorich, 2nd ed., 713–725. Boca Raton, FL: Taylor & Francis Group.

Le Bissonnais, Y. 1996. "Aggregate Stability and Assessment of Soil Crustability and Erodibility: I. Theory and Methodology." *European Journal of Soil Science* 47: 425–437.

Lee, C. H., C. C. Wang, H. H. Lin, et al. 2018. "In-Situ Biochar Application Conserves Nutrients While Simultaneously Mitigating Runoff and Erosion of an Fe-Oxide-Enriched Tropical Soil." *Science of the Total Environment* 619: 665–671.

Lee, S. S., H. S. Shah, Y. M. Awad, S. Kumar, and Y. S. Ok. 2015. "Synergy Effects of Biochar and Polyacrylamide on Plants Growth and Soil Erosion Control." *Environment and Earth Science* 74: 2463–2473.

Li, H., H. Zhu, X. Wei, B. Liu, and M. Shao. 2021. "Soil Erosion Leads to Degradation of Hydraulic Properties in the Agricultural Region of Northeast China." *Agriculture, Ecosystems and Environment* 314: 107388. https://doi.org/10.1016/j.agee.2021.107388.

Li, Q. X., Z. W. Jin, X. M. Chen, Y. Jing, Q. R. Huang, and J. B. Zhang. 2017. "Effects of Biochar on Aggregate Characteristics of Upland Red Soil in Subtropical China." *Environment and Earth Science* 76: 372.

Li, Y., G. Feng, H. Tewoldec, M. Yang, and F. Zhang. 2020. "Soil, Biochar, and Nitrogen Loss to Runoff From Loess Soil Amended With Biochar Under Simulated Rainfall." *Journal of Hydrology* 591: 125318.

Li, Y. Y., F. B. Zhang, M. Y. Yang, J. Q. Zhang, and Y. G. Xie. 2019. "Impacts of Biochar Application Rates and Particle Sizes on Runoff and Soil Loss in Small Cultivated Loess Plots Under Simulated Rainfall." *Science of the Total Environment* 649: 1403–1413.

López-Vicente, M., E. Nadal-Romero, and E. L. H. Cammeraat. 2017. "Hydrological Connectivity Does Change Over 70 Years of Abandonment and Afforestation in the Spanish Pyrenees." *Land Degradation and Development* 28: 1298–1310. https://doi.org/10.1002/ldr.2531.

Lu, S.-G., F.-F. Sun, and Y.-T. Zong. 2014. "Effect of Rice Husk Biochar and Coal Fly Ash on Some Physical Properties of Expansive Clayey Soil (Vertisol)." *Catena* 114: 37–44. https://doi.org/10.1016/j.catena.2013.10.014.

Marchamalo, M., J. M. Hooke, and P. J. Sandercock. 2016. "Flow and Sediment Connectivity in Semi-Arid Landscapes in SE Spain: Patterns and Controls." *Land Degradation and Development* 27: 1032–1044. https://doi.org/10.1002/ldr.2352.

Morgan, R. P. C., and J. H. Duzant. 2008. "Modified MMF (Morgan–Morgan–Finney) Model for Evaluating Effects of Crops and Vegetation Cover on Soil Erosion." *Earth Surface Processes and Landforms* 32: 90–106. https://doi.org/10.1002/esp.1530.

Mukherjee, A., R. Lal, and A. R. Zimmerman. 2014. "Effects of Biochar and Other Amendments on the Physical Properties and Greenhouse Gas Emissions of an Artificially Degraded Soil." *Science of the Total Environment* 487: 26–36. https://doi.org/10.1016/j.scitotenv.2014.03.141.

Mutchler, C. K., and R. A. Young. 1975. *Soil Detachment by Raindrops. In Present and Prospective Technology for Predicting Sediment Yields and Sources*, 113–117. Oxford, MS, USA: USDA Sedimentation Laboratory.

Nearing, M. A., B. Y. Liu, L. M. Risse, and X. Zhang. 1996. "Curve Numbers and Green-Ampt Effective Hydraulic Conductivities." *Water Resources Bulletin* 32, no. 1: 125–136.

Nicosia, A., C. Di Stefano, V. Palmeri, V. Pampalone, and V. Ferro. 2022b. "Evaluating the Effects of the Rill Longitudinal Profile on Flow Resistance Law." *Watermark* 14: 326. https://doi.org/10.3390/w14030326.

Nicosia, A., V. Palmeri, V. Pampalone, C. Di Stefano, and V. Ferro. 2022a. "Slope Threshold in Rill Flow Resistance." *Catena* 208: 105789.

Nicosia, A., V. Pampalone, and V. Ferro. 2021. "Effects of Biochar Addition on Rill Flow Resistance." *Watermark* 13: 3036.

Pagliai, M., and N. Vignozzi. 2002. "Soil Pore System as an Indicator of Soil Quality." In *Sustainable Land Management—Environmental Protection—a Soil Physical Approach, Advances in GeoEcology*, edited by M. Pagliai and R. Jones, vol. 35, 71–82. Reiskirchen: Catena Verlag.

Parhizkar, M., M. Shabanpour, M. E. Lucas-Borja, and D. A. Zema. 2023. "Effects of Rice Husk Biochar on Rill Detachment Capacity in Deforested Hillslopes." *Ecological Engineering* 191: 106964.

Petersen, C. T., E. Hansen, H. H. Larsen, V. Hansen, J. Ahrenfeldt, and H. Hauggaard-Nielsen. 2016. "Pore-Size Distribution and Compressibility of Coarse Sandy Subsoil With Added Biochar." *European Journal of Soil Science* 67: 726–736. https://doi.org/10.1111/ejss.12383.

Pohlmeier, A., S. Haber-Pohlmeier, and S. Stapf. 2009. "A Fast Field Cycling Nuclear Magnetic Resonance Relaxometry Study of Natural Soils." *Vadose Zone Journal* 8: 735–742. https://doi.org/10.2136/vzj2008.0030.

Pringle, C. 2003. "What Is Hydrologic Connectivity and Why Is It Ecologically Important?" *Hydrological Processes* 17: 2685–2689. https://doi.org/10.1002/hyp.5145.

Reaney, S. M., L. J. Bracken, and M. J. Kirkby. 2014. "The Importance of Surface Controls on Overland Flow Connectivity in Semi-Arid Environments: Results From a Numerical Experimental Approach." *Hydrological Processes* 28: 2116–2128. https://doi.org/10.1002/hyp.9769.

Reynolds, W. D., B. T. Bowman, C. F. Drury, C. S. Tan, and X. Lu. 2002. "Indicators of Good Soil Physical Quality: Density and Storage Parameters." *Geoderma* 110: 131–146.

Reynolds, W. D., C. F. Drury, C. S. Tan, C. A. Fox, and X. M. Yang. 2009. "Use of Indicators and Pore Volume-Function Characteristics to Quantify Soil Physical Quality." *Geoderma* 152: 252–263. https://doi.org/10.1016/j.geoderma.2009.06.009.

Risse, L. M., M. A. Nearing, and M. R. Savabi. 1994. "Determining the Green-Ampt Effective Hydraulic Conductivity From Rainfall-Runoff Data for the WEPP Model." *Transactions of ASAE* 37, no. 2: 411–418.

Risse, L. M., M. A. Nearing, and X. C. Zhang. 1995. "Variability in Green-Ampt Effective Hydraulic Conductivity Under Fallow Conditions." *Journal of Hydrology* 169: 1–24.

Russell, E. W. 1973. *Soil Conditions and Plant Growth*. 10th ed. London: Longman.

Sadeghi, S. H. R., Z. Hazbavi, and M. K. Harchegani. 2016. "Controllability of Runoff and Soil Loss From Small Plots Treated by Vinasse-Produced Biochar." *Science of the Total Environment* 541: 483–490.

Skjemstad, J. O., and J. A. Baldock. 2008. "Total and Organic Carbon." In *Soil Sampling and Methods of Analysis*, edited by M. R. Carter and E. G. Gregorich, 2nd ed., 225–237. Boca Raton, FL: Taylor & Francis Group.

Smetanová, A., M. Dotterweich, D. Diehl, U. Ulrich, and N. Fohrer. 2013. "Influence of Biochar and Terra Preta Substrates on Wettability and Erodibility of Soils." *Zeitschrift für Geomorphologie* 57: 111–134.

Sohi, S. P., E. Krull, E. Lopezcapel, and R. Bol. 2010. "A Review of Biochar and Its Use and Function in Soil." *Advances in Agronomy* 105: 47–82.

Topp, G. C., W. D. Reynolds, F. J. Cook, J. M. Kirby, and M. R. Carter. 1997. "Physical Attributes of Soil Quality." In *Soil Quality for Crop Production and Ecosystem Health. Development in Soil Science*, edited by E. G. Gregorich and M. R. Carter, vol. 25, 21–58. New York, NY: Elsevier.

Turnbull, L., J. Wainwright, and R. E. Brazier. 2008. "A Conceptual Framework for Understanding Semi-Arid Land Degradation: Ecohydrological Interactions Across Multiple-Space and Time Scales." *Ecohydrology* 1: 23–34. https://doi.org/10.1002/eco.4.

Uezu, A., J. P. Metzger, and J. M. E. Vielliard. 2005. "Effects of Structural and Functional Connectivity and Patch Size on the Abundance of Seven Atlantic Forest Bird Species." *Biological Conservation* 123: 507–519.

van Genuchten, M. T. 1980. "A Closed-Form Equation for Predicting the Hydraulic Conductivity of Unsaturated Soil." *Soil Science Society of America Journal* 44: 892–898.

Villagra-Mendoza, K., and R. Horn. 2018. "Effect of Biochar on the Unsaturated Hydraulic Conductivity of Two Amended Soils." *International Agrophysics* 32: 373–378. https://doi.org/10.1515/intag-2017-0025.

Wainwright, J., L. Turnbull, T. G. Ibrahim, I. Lexartza-Artza, S. F. Thornton, and R. E. Brazier. 2011. "Linking Environmental Régimes, Space and Time: Interpretations of Structural and Functional Connectivity." *Geomorphology* 126: 387–404. https://doi.org/10.1016/j.geomorph.2010.07.027.

Wang, J., and S. Wang. 2019. "Preparation, Modification and Environmental Application of Biochar: A Review." *Journal of Cleaner Production* 227: 1002–1022.

Wani, I., S. R. Narde, X. Huang, N. Remya, V. Kushvaha, and A. Garg. 2021. "Reviewing Role of Biochar in Controlling Soil Erosion and Considering Future Aspect of Production Using Microwave Pyrolysis Process for the Same." *Biomass Conversion and Biorefinery*: 13: 11543–11569. https://doi.org/10.1007/s13399-021-02060-1.

Warrick, A. W. 1998. "Appendix 1: Spatial Variability." In *Environmental Soil Physics*, edited by D. Hillel, 655, 771–675. CA, USA: Academic Press.

Zhang, F., C. Huang, M. Yang, J. Zhang, and W. Shi. 2019. "Rainfall Simulation Experiments Indicate That Biochar Addition Enhances Erosion of Loess-Derived Soils." *Land Degradation and Development* 30, no. 30: 2272–2286.

Zhang, P., H. Tang, W. Yao, N. Zhang, and L. V. Xizhi. 2016. "Experimental Investigation of Morphological Characteristics of Rill Evolution on Loess Slope." *Catena* 137: 536–544.